Bestrophin-3: localization and function in normal and injured tissues

Veronika Golubinskaya

Department of Physiology

Institute for Neuroscience and Physiology

Sahlgrenska Academy at University of Gothenburg

UNIVERSITY OF GOTHENBURG

Gothenburg 2015

Cover illustration: Bestrophin-3 in vasculature of mouse kidney

Bestrophin-3: localization and function in normal and injured tissues

Veronika.golubinskaya@gu.se

ISBN 978-91-628-9264-7 / 978-91-628-9265-4
http://hdl.handle.net/2077/37534
Printed in Gothenburg, Sweden 2015
Ineko AB

Bestrophin-3: localization and function in normal and injured tissues

Veronika Golubinskaya

Department of Physiology, Institute for Neuroscience and Physiology
Sahlgrenska Academy at University of Gothenburg
Göteborg, Sweden

ABSTRACT

Bestrophin-3 (Best3) is a protein with multiple functions. It can constitute a calcium-activated chloride channel when overexpressed in cultured cells, but the function of Best3 is not well studied in cells *in situ*. Recently Best3 protein was suggested to play also cell-protective role.

In this thesis the expression and function of Best3 has been studied in mouse and rat tissues by immunohistochemical methods, RT-PCR, siRNA-based downregulation and patch-clamp technique. We showed that Best3 in rat vascular smooth muscle is responsible for a cGMP-dependent, calcium-activated chloride current, important for synchronizing intracellular calcium oscillations in vascular smooth muscle cells. In mouse kidney, brain and intestine, alternative splicing produces only truncated variants of Best3 mRNA and protein which likely do not form ion channels in plasma membrane, but rather have an intracellular localization and function. These variants are expressed in mouse glomerular podocytes, in a subpopulation of astrocytes in neonatal brain after hypoxia-ischemia, and in glia-like cells in myenteric plexus of intestine. In these cells the distribution of Best3 seems to follow that of the intermediate filament nestin. Best3 is also expressed in cells of epithelial type, such as intestinal goblet cells and in brain ependymocytes. The expression of individual splice variants of Best3 changes in response to endoplasmic-reticulum-associated injury and follows separate time courses. Cultured podocytes and astrocytes after endoplasmic reticulum stress also responded with upregulation of Best3 mRNA.

It is suggested that Best3 in some cell types functions as an ion channel, whereas in other cell types it may be responding to endoplasmic reticulum stress-related cell injury. In some locations it exists in truncated splice variants; changes in the ratio between these variants may be important for the cellular response to stress. Alternative splicing may explain the variation in function of Best3.

Keywords: Bestrophin-3, alternative splicing, injury

ISBN: 978-91-628-9264-7 / 978-91-628-9265-4 http://hdl.handle.net/2077/37534

SAMMANFATTNING PÅ SVENSKA

Bestrofin-3 (Best3) är ett protein med flera funktioner. Som andra proteiner i bestrofinfamiljen kan det utgöra en kalciumaktiverad kloridkanal när det överuttrycks i cellodling, men dess funktion som jonkanal i vävnader är otillräckligt undersökt. Best3 har också nyligen förslagits spela en skyddande och antiapoptotisk roll i experiment rörande cell- och vävnadsskada i djurmodeller. Denna avhandling har undersökt lokalisationen och funktionen av Best3 i vävnader från mus och råtta. Immunhistokemiska metoder användes för att lokalisera Best3-protein, och RT-PCR samt RT-qPCR för undersökning av alternativ splitsning av Best3 i olika vävnader och för undersökningar av förändringar i uttrycket av Best3 efter cell- eller vävnadsskada. Analys av funktionen av Best3 i vaskulär glatt muskel från råtta gjordes med patch-clamp-teknik för att studera och karakterisera kalciumaktiverade kloridströmmar, och siRNA-teknik användes för att påvisa deltagandet av Best3 i dessa jonströmmar.

Best3 påvisades vara ansvarigt för en cGMP-beroende kalciumaktiverad kloridström i blodkärlsmuskel från råtta, en ström som är viktig för synkroniseringen av svängningar i den intracellulära kalciumkoncentrationen i dessa celler. I njure, hjärna och tarm från mus påvisades endast korta produkter av alternativ splitsning av Best3-mRNA. De proteiner som dessa produkter genererar kan sannolikt inte bilda jonkanaler i cellmembranen utan har sin lokalisation och funktion i cytoplasman. Hos mus uttrycks dessa i podocyter i njurens glomeruli, i en undergrupp av astrocyter i den nyföddes hjärna efter hypoxi-ischemi, och i glia-liknande celler i plexus myentericus i tarmen. I dessa celler förekommer Best3 i nära anslutning till intermediärfilamentet nestin. Best3 uttrycks också i epiteliala celler såsom bägarceller i tarmen och ependymceller i hjärnans ventriklar. Uttycket av Best3 förändras vid LPS-inducerad inflammation i njurens glomeruli och i den nyfödda hjärnan efter hypoxi-ischemi. I båda dessa modeller påvisades tecken på endoplasmatiskt-retikel-stress. Odlade podocyter och astrocyter som utsattes för thapsigargin-inducerad endoplasmatiskt-retikel-stress svarade också med uppreglering av Best-mRNA. Vid sådan skada påvisades de olika produkterna av alternativ splitsning följa individuellt olika tidsförlopp.

Best3 tycks vara inte endast en jonkanal, utan även ett led i svaret på cellskada vid endoplasmatiskt-retikel-stress, och de individuella förändringarna av de olika splitsningsvarianterna av Best3 (mätt som förhållandet mellan deras koncentrationer) kan vara viktigt för det cellulära svaret på stress. Alternativ splitsning kan vara förklaringen till att det har olika funktioner.

LIST OF PAPERS

This thesis is based on the following studies:

I. Matchkov VV, Larsen P, Bouzinova EV, Rojek A, Boedtkjer DM, Golubinskaya V, Pedersen FS, Aalkjaer C, Nilsson H. Bestrophin-3 (vitelliform macular dystrophy 2-like 3 protein) is essential for the cGMP-dependent calcium-activated chloride conductance in vascular smooth muscle cells. Circ Res. 2008 Oct 10;103(8):864-72.

II. Golubinskaya V, Elvin J, Ebefors K, Gustafsson H, Mallard C, Nyström J, Nilsson H. Bestrophin-3 is expressed in mouse glomerular podocytes (manuscript under revision)

III. Golubinskaya V, Osman A, Gustafsson H, Mallard C, Nilsson H. Bestrophin-3 is expressed in a subpopulation of astrocytes in neonatal hypoxic-ischemic brain injury (manuscript)

IV. Golubinskaya V, Gustafsson J, Gustafsson H, Mallard C, Nilsson H. Localization of bestrophin-3 in mouse intestine (manuscript)

CONTENT

ABBREVIATIONS

A7r5 – rat aortic smooth muscle cell line
BLAST – Basic Local Alignment Search Tool
BVMD – Best vitelliform macular dystrophy
CAC channel/current – calcium-activated chloride channel/current
CBF – cerebral blood flow
CFTR – cystic fibrosis transmembrane conductance regulator
cGMP – cyclic guanosine monophosphate
CHOP – C/EBP homologous protein, also called GADD153 or DDIT3
CLC, **CACL** – families of proteins-candidates for calcium-activated chloride channels
EM – electron mycroscopy
EOG – electro-oculogram
ER – endoplasmic reticulum
ERK1/2 – extracellular signal-regulated kinases 1 and 2
GABA – gamma-aminobutyric acid
GFAP – glial fibrillary acidic protein
hBest1, 2, 3, 4 – human bestrophin-1, -2, -3, -4
HEK293 – human embrio kidney cell line
HI – hypoxia-ischemia
HUVEC – human vascular endothelial cells
IF – intermediate filament
IHC – immunohistochemistry
iNOS – inducible NO synthase
LPS – lipopolysaccharide
mBest1, 2, 3 – mouse bestrophin-1, -2, -3
NFκB – nuclear factor kappa B
NO – nitric oxide
PBS – phosphate buffered saline
PCR – polymerase chain reaction
PFA – paraformaldehyde
PKG – protein kinase G
rBest1, 2, 3 – rat bestrophin-1, -2, -3

RISC – RNAi induced silencing complex
RPE – retinal pigment epithelium
RT - reverse transcriptase enzyme
SERCA - Sarco(endo)plasmic reticulum Ca2+ ATPase
shRNA – short hairpin RNA
siRNA – small interfering RNA
TG – thapsigargin
TLR4 – Toll-like receptor 4
TMEM16A – transmembrane protein 16A
TNFα – tumor necrosis factor alpha
UPR – unfolded-protein response
VRAC – volume-regulated anion channel
VSMC – vascular smooth muscle cell
WB – Western blot

1 INTRODUCTION

Ion channels regulating the flux of chloride ions are present in virtually all cells of the body and contribute importantly to the maintenance of normal body function (38). In the central nervous system, these channels are part of GABA and glycine receptors, controlling neuronal excitability and being targets for several classes of drugs, e.g. antiepileptic drugs, sedatives, and anesthetics. They regulate transepithelial transport in the kidney, inner ear, intestine, airways, and secretory glands. They are involved in bone resorption in osteoclasts and in contraction of smooth muscle and cardiac muscle. They participate in cell volume regulation and in ion homeostasis of intracellular organelles. Chloride channels can be ligand-gated (GABA-A and glycine receptors), voltage-sensitive (some CLC proteins), second messenger-activated (CFTR, calcium-activated channels) and volume-regulated (VRAC).

This thesis is focused on the second messenger-activated chloride channels, in particular those that can be activated by calcium. The calcium-activated chloride (CAC) channels are important players in regulation of cellular activity and are represented by different protein families, such as anoctamins, bestrophins, some CLC, and CACL. The first CAC currents were described in 1980s in rods of salamander retina (5). Depending on the intracellular chloride concentration, opening of these channels may lead to either depolarisation or hyperpolarisation.

1.1 Calcium-activated chloride currents in vascular smooth muscle

The presence of CAC current in vascular smooth muscle was first shown in rabbit portal vein by Byrne and Large in 1988 (17). Later a cGMP-dependent, CAC current was described in vascular smooth muscle cells from rat mesenteric arteries (55; 66; 68). Unlike for the previously known CAC currents, it was demonstrated that the new current needs activation of protein kinase G by cGMP. It has several biophysical distinguishing features from the “classical” CAC currents, such as lack of voltage dependence, linear current-voltage relation, low

sensitivity to traditional chloride channel antagonists, such as niflumic acid and DIDS and high sensitivity to blockade by Zn^{2+}. The cGMP-dependent current is activated together with the "classical" CAC currents when calcium is added intracellularly through the patch pipette, but seems to be selectively activated in mesenteric arteries by calcium released from intracellular depots by caffeine (55). This current seems to link the endothelium-dependent nitric-oxide/cyclic-GMP pathway and changes in intracellular calcium concentration, and thus plays an important role for cell coordination, coupling calcium release from the intracellular stores to changes in membrane potential. It becomes especially important in some vascular beds where nitric oxide (NO) initiates synchronized oscillations in vascular tone (61; 66). This current exists in a large number of blood vessels throughout the circulation, with the exception of the pulmonary vascular bed (56). It has also been found in intestinal smooth muscle; its function there is not yet investigated, although the link to NO could point to a role in inflammatory conditions, where it might affect bowel movement or transepithelial ion movements. A CAC current dependent on cGMP has once been described in rat renal proximal tubule cells (25) and once in cultured human airway epithelial cells (28).

The study of chloride channels, and in particular of CAC channels, is faced with difficulties. Pharmacological tools are not very selective and are generally unsuitable for experiments on whole tissues because of major side effects (most importantly opening of potassium channels). As a result, the molecular biology of the CAC channels is not firmly established. Bestrophins together with anoctamins are currently the main candidate proteins for CAC channels.

1.2 Anoctamins

Anoctamins (also called TMEM proteins, transmembrane proteins) are proteins with eight transmembrane segments expressed in cell membranes in many tissues. They were discovered more recently than bestrophins, and now anoctamins, and primarily anoctamin-1 (Ano1 or TMEM16A), attract most attention as candidates for CAC channels. When expressed in various cell types, Ano1 causes the appearance of a chloride current with properties very similar to those of endogenous "classical" calcium-activated chloride channels (19; 77; 105).

Furthermore, siRNA against TMEM16A eliminates the endogenous calcium-activated chloride current (19; 24).

1.3 Bestrophins

The family of bestrophins includes four isoforms encoded in different genes: Best1 (initially called Vmd2), Best2 (Vmd2l1), Best3 (Vmd2l3) and Best4 (Vmd2l2). In mouse Best4 is a pseudogene, but in human it seems to produce a functional protein. Bestrophins, when expressed in cells, can produce calcium-activated chloride currents with characteristics different from "classical" CAC currents (73; 89). Bestrophin proteins have a conserved sequence between different isoforms and between different animal species (so called bestrophin domain), but the C-terminus varies substantially between isoforms and species (Fig.1). The bestrophin domain sequence is predicted to contain four transmembrane domains, while the N- and C-terminal parts of the proteins are localized intracellularly (37).

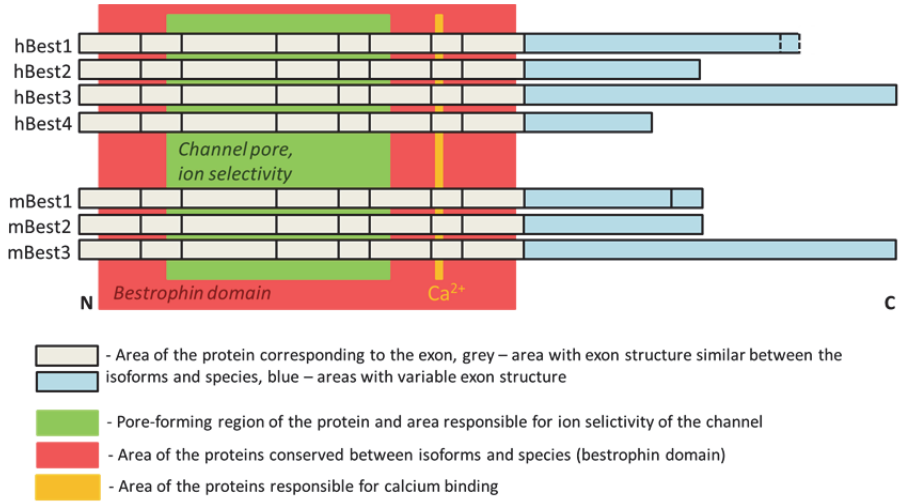

Fig.1 ***The structure of mRNA and protein for different bestrophin isoforms in human and mouse****. All bestrophins show high similarity in exon structure in a conserved bestrophin protein domain which includes transmembrane loops forming a channel pore and a calcium-sensing area. The C-terminal area of the bestrophin proteins is more variable between isoforms and species and can correspond to 1 or more exons.*

The first described bestrophin, human Best1 (hBest1), was found as the gene responsible for mutations associated with Best vitelliform macular dystrophy, or Best's disease (BVMD) (67). Mutations in hBest1 were also found in some cases of adult-onset vitelliform macular dystrophy, Bull's eye maculopathy and autosomal dominant vitreoretinochoroidopathy (37). hBest1 is expressed in retinal pigment epithelium (RPE), the layer of pigmented epithelial cells on the outer side of retina. The RPE regulates the fluid surrounding photoreceptors and provides regeneration and phagocytosis. In the case of BVMD large deposits of yellow pigment (lipofuscin) are formed in sub-RPE and subretinal spaces, the RPE layer becomes thickened and the retina above it becomes thinner, photoreceptors degenerate and the vision deteriorates. BVMD is characterized by an abnormal electro-oculogram (EOG). EOG reflects transepithelial potential, which appears over RPE cells as a result of polarized distribution of ion channels between apical (facing the photoreceptors) and basolateral (facing the choroid) side of the cell membrane. This voltage difference increases during light stimulation, and the maximal voltage in the light is called the light peak. The light peak is considered to be a result of depolarization in the basolateral membrane of the RPE caused by an increased chloride conductance probably due to Best1 expressed in the basolateral membrane of the RPE or intracellularly in association with RPE membrane and acting as chloride channels or as regulators of other channels (87). BVMD is a multifactorial disease, and mutations of hBest1 gene and protein are very likely involved (37). At the same time, Best1-knock-out mice do not have retinal pathology, which might mean different function of ocular Best1 in human diseases and in mouse models (52; 54). Because of its connection to human retinopathies, the Best1 isoform is the most studied compared to the other bestrophins.

Previous studies have suggested bestrophins to form a channel as multimers (89) consisting of homomers, where the same bestrophin isoform participates in channel formation (11). Recently the structure of bestrophin channels was described based on a crystallized structure of a bacterial homolog of human Best1 (104) and on the X-ray structure of chicken BEST1-Fab complexes (40). Based on these experiments, the Best1 channel is a pentamer forming a "flower vase" shaped channel structure with a surface-charged pore. Each monomer has four transmembrane parts with short extracellular loops between

transmembrane domains 1-2 and 3-4 and with a long intracellular loop between domains 2-3. N- and C-terminals are facing the intracellular side and form an intracellular channel cavity.

The ion selectivity area of bestrophin channels is localized in transmembrane domain 2 (95) in the narrowing ("neck") of the channel (40; 104) and is restricted to a few amino acid residues, modification of which can dramatically change ion permeability and selectivity of the channel. The point mutations in human Best1 previously described in relation to human retinopathies are localized primarily in the neck area of the channel.

The calcium sensitivity of bestrophins is in the lower range of physiological concentrations of intracellular calcium. hBest1 is activated by calcium with Kd around 150 nM, and basal free cytosolic calcium concentration is usually around 100 nM (37). Bestrophins can be activated by calcium directly, but this activation can be accelerated by adding ATP (21). The conserved area of the bestrophin proteins responsible for calcium sensing (300)EDDDDFE(306) is localized in the C-terminus directly after the last transmembrane domain and consists of negatively charged amino acids (21; 94). This area in hBest1 is similar to the calcium-binding loop of calmodulin and troponin C (101) and has some similarity to the calcium bowl of big-large-conductance (BK) potassium channels (37). The calcium-sensing area in hBest1 stays in close contact with the intracellular loop (40; 104). It was suggested that binding of calcium would widen the "neck" part of the channel and let the ions pass through (40).

The functions of bestrophins are still not fully understood and may vary between different tissues. Mouse models for genetic knock-out of Best1 and 2 did not show obvious phenotypical pathologies (6; 52; 54). There is clear data that hBest1 is important for the functioning of RPE in human eye, and this is likely connected to its channel activity (see above). Best2 in the mouse eye is not present in RPE, but instead is expressed in nonpigmented epithelia and there participates in regulation of intraocular pressure (6). There is also data that bestrophins might act as stretch-activated or volume-regulated anion channels (VRAC): the currents induced by expression of hBest1 and mBest2 can be inhibited by hyperosmotic and stimulated by hypoosmotic solutions (32). Thus it is likely that bestrophins can

participate in the regulation of cell volume and in other cell functions connected with VRAC activity, such as control of the cell cycle, mechanotransduction and apoptosis (37). In olfactory sensory neurons mBest2 is proposed to induce CAC currents which are responsible for amplification of the response and for olfactory receptor potential (37).

Even if bestrophin channels are confirmed to be chloride channels, variations in their ion selectivity in different cells are not fully understood. Human bestrophins 1, 2 and 4, and mouse Best2 (mBest2) were shown to be highly permeable for bicarbonate when expressed in HEK293 cells (72). Another study gives indirect evidence that mBest2 can function as a bicarbonate channel in goblet cells in mouse colon (106). Other data suggest that Best1 can pass GABA in cerebellar glia cells (48) and probably in meninges and choroid plexus epithelial cells (93) or can be permeable to glutamate (63).

Bestrophins (especially Best1 and 3) are widely expressed in different tissues and are reported to be present in brain, eye, exocrine glands, heart, vasculature, intestine, kidney (27; 37), but most of the data is based on mRNA expression analysis. The attempts to visualize bestrophins within cells have given quite contradictory data, and studies have shown a likely cytoplasmic localization for human and mouse Best1 (8; 60). In this case they can be either intracellular ion channels or intracellular regulators. It was suggested that in epithelial cells Best1 is localized in the endoplasmic reticulum and provides a current of counter-ions during release of calcium (8; 60). There are also observations that hBest1 localizes intracellularly close to the plasma membrane and regulates the activity of voltage-gated calcium channels of the plasma membrane by an interaction of hBest1 C-terminus with the β-subunit of L-type calcium channels (57; 76; 107).

There is also data suggesting that bestrophins are involved in processes of cell survival, cell division and tissue repair. In chemosensory neuroepithelia mBest2 is suggested to participate in differentiation and growth of axons and sensory cilia (44). A high level of expression of Best1 is associated with fast growth in T(84) colonic carcinoma cells (84). Best1 in mouse renal collecting duct cells can increase cell proliferation and participate in epithelial-to-mesenchymal transition (4). There is also data about anti-apoptotic functions of Best3

which will be discussed in more detail later. It is questionable whether these functions depend on the ion channel function of bestrophins.

1.4 Bestrophin-3

The Best3 isoform is much less studied than Best1. The Best3 protein shares much similarity with the other bestrophins in its N-terminal transmembrane part and in the calcium-sensing area, and differs from the other isoforms by having a longer intracellular C-terminal part.

When expressed in cells, Best1 and 2 always induce a CAC current characteristic for bestrophins. However, even if overexpressed mBest3 protein was introduced into cell membrane, it only produced a small CAC current (85). In other experiments mBest3 and hBest3 in their native form were not able to produce CAC current (73), but the channel could be opened, and current recorded if a definite area in Best3 C-terminus was mutated or if the whole C-terminus part distal from residue 353 was deleted (73). This area, (356)IPSFLGS(362), was suggested to be an autoinhibitory domain for the Best3 channel. It is surprising that overexpressed Best3 channel in these two similar experiments (in both cases mBest3 was overexpressed in HEK cells) could be either active or inactivated, and probably the same situation takes place *in vivo*. Best3 was also shown to form a functional CAC channel in mouse cardiomyocytes where it seems to exist in an activated state (62).

Best3 mRNA can undergo alternative splicing, and as a result truncated splice variants of Best3 protein can be produced. Alternative splicing of Best3 was mostly studied in mice (45; 85), but different variants of human Best3 mRNA are reported in databases and in (86). Recently alternative splicing was shown also for Best1 (47). As a result of alternative splicing of mBest3 mRNA, the exons 2, 3 and 6 can be excised in different combinations in different tissues. All these exons encode protein areas predicted to be transmembrane loops involved in forming the channel pore and responsible for channel permeability and selectivity. Among the mouse tissues studied only heart tissue was shown to have full-length Best3 mRNA so far (45), and Best3 splice variants are very little studied on the protein level. When expressed in cells, the most spliced variant of Best3, missing all

three exons ("-2-3-6"), showed no current even though it targeted the plasma membrane, while the full-length mBest3 variant in the same experiments produced CAC current (85). It is quite expected that these splice variants of Best3 may not be able to function as transmembrane proteins and ion channels, but at the same time the transmembrane loop located in exons 6 and 7 and the other hydrophobic areas in the protein probably can still provide some connection of the protein to a membrane – whether plasma membrane or intracellular.

Recently the Best3 isoform was reported to have anti-apoptotic and cell-protective functions, which previously had not been described for bestrophins. In rat basilar artery smooth muscle cell culture siRNA based knock-down of Best3 resulted in increased H_2O_2-induced cell death, and overexpression of Best3 prevented cell apoptosis (39). Authors suggest that this antiapoptotic effect of Best3 is associated with stabilization of membrane potential in mitochondria, decrease in caspase-3 activation and cytochrome c release and with changes in Bcl-2/Bax ratio. In cultured rat renal epithelial cells Best3 protects cells from death induced by endoplasmic reticulum (ER) stress (49). In this ER stress model the increase in Best3 expression was induced by activation of ERK1/2, and Best3 was further suggested to downregulate CHOP – a protein marker associated with cell apoptosis in ER stress. In human vascular endothelial cells (HUVEC) Best3 also seems to participate in inflammatory responses and inhibits NFκB pathway activation in response to TNFα (83). All these publications are different and single, use different models of injury and are mostly done in cell culture models from different species, but all suggest that Best3 can have a cell-protective role.

In this thesis we were interested in the expression and function of Best3 in relation to its suggested chloride channel functions and to its possible involvement in cell protection. As there is very little data on expression of Best3 protein *in vivo*, we were interested to detect it in different tissues in rodent models. Best3 gene expression may cause multiple variants of the Best3 proteins to appear as a result of alternative splicing of Best3 mRNA, so we also focused our research on alternative splicing for Best3 in different tissues and its regulation in the situations of tissue and cell injury.

2 AIMS

- To study Best3 expression in different tissues (vascular smooth muscle, kidney, brain, intestine) in rodents;

- To study Best3 localization in certain cell types;

- To investigate if Best3 is responsible for calcium-activated chloride channel in vascular smooth muscle;

- To study alternative splicing of Best3 mRNA;

- To study expression of Best3 splice variants in relation to tissue and cell injury

3 METHODS

3.1 Animals used in the studies

The experiments were performed in male Wistar rats (Paper I) and in C57Bl6 mice of either sex (Paper III, IV and in Paper II in experiments with immunochistochemical detection of Best3 in glomeruli) or in male C57Bl6 mice (Paper II in experiments with LPS administration). No difference in expression of Best3 was observed between male and female mice. When quantitative analysis of Best3 mRNA expression was performed in the mixed-gender groups (Paper III), each group had equal representation of males and females.

In Paper I, II and IV most of the experiments were performed on adult animals, though in Paper II and IV some immunostainings were made also in immature kidney and intestine of mouse pups at postnatal day 10. Paper III describes the study of hypoxic-ischemic brain injury in neonatal mice, but additional experiments detecting Best3 presence in uninjured brains of adult mice were also performed.

3.2 Cell cultures used in the studies

Cell culture is a commonly used tool to study structure and function of proteins on the cellular level. Cells can be cultured as primary cells, when they are obtained directly from the tissue, or can be further immortalized - genetically modified to be able to proliferate indefinitely. Primary cell cultures are considered to be in a more natural state than the immortalized cells, but can be used only in a limited number of passages while they keep the characteristics of the original cells. Immortalized cells are stable through many more passages, but genetic modifications can influence some of the cell functions.

Cell culturing approaches allow different treatments which are either not possible or too severe in studies in the whole animal. Compared with whole tissue homogenate, cell culture gives a homogenous material where only one or mostly one type of the cell is

present, so it is easier to connect the function of interest to a particular cell type. Experiments in cell culture often give reproducible results, and it also expands the possibilities for research in humans as live cells for culturing can be obtained from surgical material or biopsies.

At the same time, working with cell cultures has restrictions, as most of the cells are in an "unnatural" state while cultured alone or on artificial, commonly, flat substrate. It is of particular importance for highly differentiated cells with developed cell architecture and space-oriented cell-to-cell contacts. There are advanced techniques to imitate the natural cell environment, such as co-culturing of different types of cells as well as using various kinds of surfaces for cells to grow on (different coating to help attachment of the cells or even 3D-oriented surfaces). However, conclusions from cell culture-based experiments should be made with caution, and should be confirmed by experiments on whole animal as much as possible, or at least on the level of isolated organs/tissues. Used in this way, cell culture is a powerful tool which also allows reducing the number of animals used for the research.

Rat aortic smooth muscle cell culture A7r5 (Paper I)

A7r5 is a clonal cell line obtained from smooth muscle myoblasts of rat embryo aorta by using the method of "selected serial passage" (43). The cells have the phenotype of smooth muscle cells confirmed by electron microscopy and can produce spontaneous action potentials synchronized between the cells, which shows that the cells are electrically coupled (43).

Immortalized cell culture of mouse podocytes (Paper II)

Culturing of primary podocytes leads to rapid de-differentiation and loss of cell processes and of expression of synaptopodin, the marker for differentiated postmitotic podocytes. Avoiding repeated subcultivation improves podocyte culturing, but in those cultures podocytes still stay only partially differentiated (58). Later P.Mundel and co-authors have introduced a method to culture immortalized mouse podocytes with improved differentiation properties (59). These cells originate from outgrowth from isolated cultured glomeruli of a transgenic mouse expressing tsA58 (temperature-sensitive SV40 large T antigen) under the interferon-γ inducible promoter. These cells are immortalized and can proliferate at high rate under permissive conditions (33°C, presence of interferon-γ). In non-permissive

conditions (37°C without interferon-γ) they become growth arrested and differentiate into cells forming cell processes, and even slit-diaphragm-like cell-to-cell contacts, and also start expressing most of the differentiated podocyte markers (78). The podocyte cell culture used in our experiments was a kind gift from P.Mundel.

Primary culture of mouse astrocytes (Paper III)

Mouse astrocytes were obtained from newborn mouse brain homogenates (postnatal day 1-3) first as a mixed culture of all primary glial cells (astrocytes, oligodendrocytes and microglia). After the cells reached confluence in cell culturing flasks, the culture was left shaking overnight, so that most of microglia and oligodendrocytes detached and were later removed. The still attaching cells consist of up to 98% of astrocytes (26). Cells were detached from the bottom of the flasks by trypsination and reseeded into 12-well plates for qPCR analysis or to the glass slide chambers for immunostaining.

The majority of the cells were positive to astrocyte marker GFAP. As the cultures were not completely pure, treatment used may have influenced not only astrocytes, but also microglia. Thus the responses from the astrocyte cultures could be a result of direct effects of the treatment on astrocytes and/or indirect effect of other active substances secreted by affected microglia.

3.3 Methods of detection of Best3 in different tissues

New protein can be detected in the tissue or in the cells first on the level of protein itself (antibody-based approaches, protein mass spectrometry etc.), but also on the level of its mRNA (reverse-transcriptase based RNA detection, hybridization of RNA with specific probes etc.) or detecting of its function, if it is known. While cell culture, as a homogenous material, often gives more clear results, methods to detect protein in tissue always have to deal with different types of the cells present in the sample. In the case of protein detection in the tissue, direct visualizing of the protein or mRNA is of special importance for characterizing which cells are expressing it. In immunochemical studies characterization of the positively stained cells

can be done on the basis of their morphology and by co-localizing the protein of interest with other proteins, such as specific cell markers for different cell types.

When methods require homogenization of the tissue sample, the sample can be enriched with the cells of interest and compared to the native homogenate. For example in Paper II we used glomeruli-enriched fraction of mouse kidney by a previously developed method (58). This fractionation produced samples containing about 80-90% of glomeruli, which contained enough material for mRNA extraction with regular RNA-purification kit and was quick enough to keep good quality of mRNA in the samples. An alternative method could have been manual dissection of glomeruli from kidney samples, but because of the small size of mouse glomeruli it would be technically very difficult and the sample yield would be low.

As the protein function is usually a major target of the study, it is not enough to show the expression only on the level of mRNA, as mRNA is not always fully translated to protein, and it is thus important to show also the presence of the protein product in the sample. At the same time, while studying the time course of changes in protein expression and its regulation, mRNA analysis is a powerful, quick and quantitative tool to study the early processes, which later may lead to changes in protein expression and function. The study of truncated variants of the same protein due to alternative splicing of mRNA should also start from mRNA analysis, as developing antibodies is much more difficult and limited than construction of PCR primers.

3.3.1 Protein detection

Antibody-based techniques: Immunohistochemistry (Paper II, III and IV) and Western blotting (Paper I, II, IV)

Immunohistochemical methods of protein detection are based on recognition by a primary antibody of a specific antigen region in the protein against which the antibody has been developed. Primary antibodies can be labeled and seen by fluorescence or chromogenic detection methods directly or more commonly can be revealed by labeled secondary antibody. Fluorescent methods are used when experiments aim at co-localizing several protein targets in the same

specimen, or when high resolution microscopy, for example confocal microscopy, is performed. In our experiments (Paper II, III and IV) we mostly used immunofluorescent methods, but also horseradish peroxidase-based chromogenic immunodetection as an alternative method to visualize Best3 in the tissues (Paper II and IV).

Primary antibodies are raised by injecting the animal with antigen, either the full protein of interest or more often a part of it. Selection of the antigen area within the protein of interest depends on the needs (for example to have extracellular or intracellular binding in the case of transmembrane protein), but is restricted by secondary structure of the native protein. Polyclonal antibodies are produced by a mixture of different immune cell lineage and sometimes recognize several epitopes within antigen. In contrast, monoclonal antibodies are produced by a single clone of immune cells and recognize only one epitope on the antigen.

Even if antibodies (primary or secondary) recognize antigen with high specificity, the possibility of unspecific binding to similar sequences in irrelevant proteins cannot be excluded, especially in cases of low expression of the protein of interest. If possible, more than one primary antibody against the protein of interest should be used. To avoid false-positive results one should control the specificity of the antibody first by performing a search for the antigen sequence in protein databases available on-line to see if the sequence exists only in the protein of interest. In the studies in this thesis the BLAST (Basic Local Alignment Search Tool) from http://blast.ncbi.nlm.nih.gov/Blast.cgi) database was used. It is not always possible to perform a BLAST analysis prior to using an antibody, for example in case of commercial antibodies when the company refuses to provide the information about the antigen sequence. Another important controlling step for false-positive staining is to use a blocking peptide – a peptide with a sequence identical to the antigen. In this method, the blocking peptide is incubated with the antibody so that the antigen-recognizing area of the antibody will be blocked. The possible unspecific binding of secondary antibodies can be controlled by excluding the primary antibody from the incubation buffer, thus the secondary antibody should not have a target to bind to. Such experiments will also help to exclude unspecific signals coming from autofluorescence or from endogenous peroxidases. In the case with fluorescent labeling,

autofluorescence can be controlled by having a specimen that was not exposed to the secondary antibody and by running the same experiments with different colors of the label dye.

In our experiments we used a commercial polyclonal anti-Best3 antibody that was made against mouse Best3 antigen. The company provided us with information about the antigen sequence, and the BLAST analysis confirmed that the antigen was localized in the intracellular part of Best3 protein at the very end of the C-terminal part. Splicing of the C-terminal part of mouse Best3 has not been reported so far, so we expect that the antibody used in this thesis does not distinguish between Best3 splice variants neither in the immunochemical analyses nor in Western blotting, while this was not specially studied. The BLAST analysis also showed that the Best3 antibody is highly specific to recognize only the Best3 isoform, has few mismatches in recognizing corresponding area in rat Best3 protein and cannot recognize human Best3, corresponding to the published human Best3 sequence. It was not possible for us to find another satisfactory commercial anti-Best3 antibody for experiments in the mouse, but the blocking peptide corresponding to our anti-Best3 antibody was available for purchase and proved the specificity of it by eliminating the staining in tissues and cells (Paper II, IV).

For the efficiency and quality of immunochemical protein detection it is very important to use an appropriate method of fixation to stop the cellular processes at the moment of interest and to prevent degradation of cellular proteins or changes in their placement within the cell. The most widely used methods to preserve cell morphology and protein integrity are fixation with aldehydes, commonly paraformaldehyde (PFA) or glutaraldehyde, with acetone and alcohols or preservation of non-fixed samples by freezing.

Aldehydes fix the sample by cross-linking the proteins within the cells by building covalent chemical bonds between amino acids residuals. In this case small or soluble proteins get anchored to large proteins of cytoskeleton, which keeps them in place and preserves cell integrity. Paraformaldehyde is used as a solution in phosphate-buffered saline (PBS) at different concentrations (usually from less than 1% up to 10%) to get different strength of fixation.

Acetone and alcohols (commonly methanol, ethanol or their mixture) are denaturing or precipitating fixatives. They make proteins less soluble and can also facilitate the release of proteins from hydrophobic interactions and thus denature the secondary structure of the protein. Freezing of native specimens is a quick way to preserve the sample. For further immunostaining, the frozen samples usually still require fixation to prevent protein degradation, which can be performed quickly and efficiently on cryostat sections of the sample.

All methods of fixation have their strong and weak points. Fixation by freezing is very quick and should be used in the case of quickly degrading or changing proteins, for example in studies of enzymes, proteins with short life time, protein phosphorylation or protein-protein interactions. The tissue morphology is often not well preserved after freezing, as the ice crystals forming in the tissue can mechanically break up the structure. It is very important to freeze the samples quickly and evenly, which can be a problem for bigger samples. Cryostat sectioning can be difficult sometimes, depending on structural properties of the tissue, and it is difficult to make cryostat sections very thin, which can be a problem when slow penetrating antibodies are used. At the same time frozen sections usually have higher sensitivity to antibodies than paraffin-embedded tissues, which can compensate for the loss in antibody penetration.

Denaturing fixatives do not create extra bonds between proteins (as aldehydes do), but rather denature the secondary structures of the proteins making the antigens available for detection by the antibody. At the same time this can be a problem if the protein secondary structure is necessary for antibody recognition. Further, denaturing fixatives can dissolve hydrophobic cell structures, such as plasma membrane and intracellular membranes of organelles, which can influence cell integrity and morphology and loss of membrane-associated proteins.

Aldehydes are good for preservation of tissue morphology and native structure of the proteins. Fixed samples are easy to work with, can be easily embedded in hard materials, such as paraffin, and further can be stored and processed at room temperature. Tissue samples can simply be placed in the PFA solution until it is fixed, as it is usually done for example with human biopsies or in animal research when

small tissue samples from the same animal will be used for different purposes. However, for bigger samples penetration of the fixative can take several hours, so the tissue can start degrading. In such cases perfusion-fixation is advantageous, as the fixative is transcardially infused under pressure into the blood stream of the animal, and the cells in the tissue are getting in contact with the fixative faster and more evenly. Perfusion-fixation can also be important for preservation of vascular structure.

At the same time in experiments with fluorescent detection, the presence of aldehydes in the tissue can increase autofluorescence. Another disadvantage with aldehyde fixation is that the cross-linking between different proteins or within the same protein can cause masking of the antigen area if it participates in protein-protein interactions and in formation of the secondary protein structure. In this case antibodies might not be able to find and recognize the antigen area. One possible solution to antigen masking by aldehydes is a standard procedure of antigen retrieval, where the specimen is heated in citrate buffer with either pH 6.0 or pH 8.0 (80; 81). During this procedure disulfide bonds between amino acids are destroyed, and the antigen area hidden by fixation or by native secondary protein structure, can be revealed. Still not all cross links between amino acids can be destroyed, and hidden antigens cannot always be revealed, but chances for success are higher if the percentage of aldehyde in fixative is lower, temperature during antigen retrieval is higher, and the duration of it is longer. Antigen retrieval can influence the tissue morphology and can also become a problem in the experiments when more than one antibody is used, as recognition of antigens by other antibodies or stains may actually require secondary structure of the protein to be intact. Sometimes partial digestion of proteins in the sample by short incubation with proteinase K can also help to retrieve antigens.

In our experiments the anti-Best3 antibody required antigen retrieval after PFA fixation. The best results were achieved when paraffin-embedded samples were heated for 20-30 min at 97°C in 0.05M citrate buffer at pH 6.0. Percentage of PFA in fixing solution and time of incubation was crucial: antigen could not be retrieved in the tissue samples which were fixed with PFA higher than 4% or were incubated with PFA for longer than 2 days. The best results were

obtained by incubating the samples with PFA at 4°C, as incubation at room temperature increased autofluorescence in the tissues and decreased signal-to-noise ratio. Our anti-Best3 antibody seems to have slow penetration ability, as the optimal incubation time was 2 days at 4°C, incubation for shorter time at room temperature decreased signal-to-noise ratio. As the antibody was created against an intracellular antigen region of Best3, permeabilization of the cells with detergent was necessary for tissue and cell culture samples. Having detergent in antibody incubation mix for longer time also helped to improve the staining in tissue samples probably due to increase of antibody penetration into the tissue.

Another difficulty working with the anti-Best3 antibody was co-localization of Best3 with different cell type markers. To perform such studies the primary antibodies used for co-localization should be originating from different host animals, so that different secondary antibodies, labeled with different dyes, can recognize each primary marker independently in the same sample. The anti-Best3 antibody used in this thesis is raised in rabbit, which is a very commonly used host animal, especially for the antibodies against mouse proteins. Even if the commercial market for antibody production is very developed, it was surprisingly difficult to find IHC-compatible cell markers made in other host animals than rabbit.

Western blotting (WB) technique is also based on antibody-antigen recognition, while total proteins are extracted from the tissue or cell culture sample. The proteins are usually denatured to break protein-protein interactions and secondary protein structure, and then separated on a gel by electrophoresis corresponding to their molecular size. Further proteins are transferred from the gel to a nitrocellulose membrane and there stained with antibody. This should reveal a band corresponding to the predicted weight of the studied protein in accordance with the standard molecular weight ladder. Often several antibody-positive bands can be detected. It can be due to the unspecific binding of the antibody, but it can also be specific and give additional information. The heavier bands may indicate the presence of posttranslational modifications of the protein (for example glycosylation) or even in some special circumstances protein-protein interactions when protein of interest keeps its boundaries to the other protein(s) and travels through the gel as one protein complex. Lighter

bands than expected, very often reflect protein degradation during sample processing, but can also show presence of functional short fragments of the protein for example as a result of alternative splicing or regulatory cleavage of the protein. Antibodies not working well and specifically in immunohistochemical experiments, can sometimes be used successfully in WB, and vice versa, as in the first case proteins stay in more natural surroundings and keep a more native structure, while the proteins are in a denatured state in WB analysis.

Compared with immunohistochemistry, WB is more often used for comparative quantification of protein expression in situations with treatments or pathologies. However, if WB is performed in tissue homogenate, it shows the change of total protein from all of the cells in the tissue, and additional experiments with cell culture or homogenates enriched with one type of the cells are often required. Immunochemistry allows distinction of protein expression in different cell types, but quantification is often difficult and time consuming. For detailed characterization of protein expression in tissues, these techniques are complementary. In our experiments with WB we used a standard NuPage-SDS protocol. It was difficult to study separate splice variants for Best3 based on multiple bands on the WB gel, as the difference in molecular weight between the bands was only 2.5 – 3 kDa, and also the possibility of posttranslational modification of the Best3 proteins cannot be excluded.

Immunogold-based detection of Best3 protein by electron microscopy (EM) (Paper II)

EM techniques allow studying samples with very high resolution compared to light microscopy, so they can be used to visualize structure at a subcellular level. Immunogold EM techniques use the same principle as that previously described for immunochistological methods and are based on recognition of antigen by primary antibody. Further the primary antibody is recognized by gold particles-labelled secondary antibody or immunoglobulin G-recognizing protein A. A transmission electron microscope is commonly used for detection of immunogold staining. It irradiates the specimen with a beam of accelerated electrons and visualizes electron-dense gold particles scattering electrons from the beam as black dots in the image.

Traditionally EM techniques are considered to be difficult, time consuming and not easy to succeed with. The result depends drastically on preservation of the tissue structure as well as on the efficiency of the antibody. Successful analysis also depends on the expression level of the protein of interest. The specimens used for EM are usually very thin (nanometer range) compared to traditional microscopy (micrometer range), and magnification of the image is higher, thus fewer protein molecules exist per image. For sectioning, the specimens are embedded in hard materials (often different kinds of resin) or can be frozen. The frozen sections very often have less well preserved cell structure and cannot be cut as thin as resin-embedded samples, but the sensitivity of the antibody usually is higher in frozen tissue samples. In our experiments we needed to keep the antibody sensitivity high, but we also had to have as good preservation of the tissue structure as possible. In order to achieve this we combined PFA-fixation of kidney tissue with cryosectioning after sucrose cryoprotection of the samples. To optimize the staining with the Best3 antibody, we also introduced citrate antigen retrieval procedure into the protocol.

3.3.2 mRNA analysis

Extraction of mRNA from tissues and cells

mRNA (or messenger RNA) transforms the information from a gene to a protein product. The full-length mRNA sequence corresponding to the protein of interest can be predicted on the base of exon-intron structure of the gene and further confirmed by nucleotide sequencing. Not always all mRNA produced in the cell is translated to protein, but still most often changes in mRNA level cause changes in protein expression. Regulation of mRNA expression occurs prior to changes in protein level, and the delay of the protein response can be quite pronounced in case of slow synthesis and turnover of the protein.

To extract mRNA from tissues we used the silica membrane-based total mRNA purification kits from Qiagen. Selection of specific kit types depended on the tissue type or the sample size. RNA can be easily destroyed by RNases present in the tissues and the cells, so RNA purification procedures should be performed quickly and clean, and during sample homogenization the use of RNase-eliminating agents is

beneficial. In our experiments with cell cultures, with tissues and glomeruli-enriched fractions we used a standard RLT homogenizing buffer containing 1% of beta-mercaptoethanol which eliminated RNases by reducing their disulfide bonds. It is also important to efficiently eliminate genomic DNA (gDNA) from the mRNA samples, as gDNA contamination of cDNA can be a problem for further PCR analysis. This can be done by incubating the mRNA sample with DNase, which recognizes and digests only DNA, but not RNA sequences. In our experiments we always performed gDNA digestion prior to RT reaction.

RT-PCR, quantitative RT-PCR and primer construction (Paper I, II, III and IV)

After mRNA has been extracted, it can be either analyzed directly or, as in our experiments, the DNA sequence complementary to the mRNA sequence (cDNA) can be generated. This is performed by incubating the mRNA sample with reverse transcriptase enzyme (RT) of viral origin, which produces cDNA in 1:1 ratio to the original mRNA. Usually when we analyze mRNA expression of a specific gene by RT method, as a result of RT reaction we get the sample containing different cDNA representing all mRNA existing in the sample.

The further polymerase-chain reaction (PCR) analysis is called *RT-PCR*, as it uses a product of reverse transcription as a template. Sometimes the term "RT-PCR" is used as another name for quantitative PCR meaning "Real-Time PCR", but it would be more correct to call it "real-time RT-PCR", "quantitative RT-PCR" or just "qPCR" in the case of cDNA used as a template. PCR is a way to exponentially amplify DNA by DNA polymerase starting sometimes from one or few DNA molecules and ending up with billions of copies. mRNA expression analysis by PCR requires amplifying only the cDNA corresponding to the mRNA of interest, so the amplification is based on specific primers annealing only to the specific sequence in the cDNA of interest.

Quantitative RT-PCR (qPCR)

qPCR is a variant of RT-PCR that allows quantification of the amount of template cDNA in the sample. The detection of DNA occurs in "real time" – in every PCR cycle when the new DNA strands are produced by polymerase. The reporting molecules are either unspecific

fluorescent dyes, which interact with all double-stranded DNA in the sample, or fluorescent-labeled sequence-specific DNA probes recognizing only the amplification product of interest. qPCR based on detection with the specific probes is more expensive and requires an additional step of probe construction, but it gives more precise quantification of cDNA as it does not recognize unspecific DNA in the sample, such as primer dimers. It also allows quantification of cDNA for several PCR products of interest simultaneously. Commercial probes to detect Best3 splice variants were not available. Based on published data we constructed primers for the different Best3 splice variants (see below) and used a qPCR protocol with the fluorescent dye SYBR Green as a reporter. These pairs of primers were tested before experimentation and found to be reliable (Fig.2). As the control for unspecific detection of primer dimers we used a blank sample containing no cDNA template. We also analyzed the melting curve of the PCR products in the end of each qPCR run.

For correct quantification of cDNA it is important to control the individual differences between the samples appearing as a result of different quality of mRNA in original samples, variations in efficiency of RT reaction and variations between different qPCR runs. For that purpose normalization of the qPCR values for the gene of interest to the values for house-keeping gene(s) is used. House-keeping genes are highly expressed in the studied tissue, and when the results of treatment are studied on mRNA level, the house-keeping gene should not have pronounced changes in its expression in response to the treatment. It can be challenging sometimes to find satisfactory house-keeping genes, and very often in different situations different house-keeping genes are used. In our experiments we used GAPDH in Paper I, III and IV, but in the experiments in Paper II Gusb was more appropriate.

Construction of specific primers for RT-PCR

It is a very important step in the study of mRNA expression. Primers should be efficient in the amplification reaction, and the possibility of unspecific recognition of irrelevant substrates by the primers should be minimalized. DNA polymerase can amplify DNA strands only in the direction from 5’ to 3’, so to construct the forward primer for Best3 we use the sequence of 5’-3’ strand of genomic DNA for mBest3 which is published in gene databases, and for reverse

primer – its complementary sequence. The amplified area is located between forward primer on 5' end and reverse primer on 3' end. The most common rules to select the primer sequence are:

- If possible, forward and reverse primers should anneal in different exons. Then in the case of residual gDNA contamination in the sample, amplification of genomic DNA will be inefficient (if the intron area between the exons is long enough) or unspecific amplification will be seen as multiple bands or a smear lane on the gel (if the intron is short and can be amplified);
- The sequences of the primes should be checked online by BLAST analysis (http://blast.ncbi.nlm.nih.gov/Blast.cgi). Usually such short RNA sequences, when blasted separately, can have a high level of unspecific recognition, so it is important to blast the primers together as a pair (http://www.ncbi.nlm.nih.gov/tools/primer-blast). In this case we can see if both forward and reverse primers recognize the area within the same irrelevant gene and produce unspecific products in the PCR;
- The length of the primers is usually 18-24 bp. The shorter primers tend to be less specific as the shorter the fragment is, the higher are the chances to find this sequence in an irrelevant gene. However, longer primers will have less efficiency in the PCR runs;
- The primer sequences should not have complementary areas within the same primer or between forward and reverse primers, as this may reduce the efficiency of the primer pair in a PCR run due to formation of primer dimers or loops within the primers;
- The sequence of the primer should not have too high content of G and C nucleotides (optimal 40-60%), as these nucleotides form stronger complementary bonds between each other compared to A-T bonds. Primers with high G/C content require higher melting temperature in the PCR run which may cause reduced efficiency of the PCR. It is important that forward and reverse primers in a primer pair have similar melting temperatures.

There are many commercially available primers, and we used some of them to detect mRNA for nestin, CHOP and housekeeping genes. However, it was a problem to find satisfactory primers to detect Best3, as the selection of commercial primers for Best3 was fairly poor and very often primer pairs were made without considering the alternative splicing of Best3 mRNA. In order to overcome these limitations, we

constructed our own primers for detection of all Best3 splice variants. There are many possibilities to create primers using special software, including free-access online services. For construction of Best3 primers we mostly used software from Jellyfish 3.3.1 (Field Scientific, LLC, USA) and ncbi primer BLAST tool (http://www.ncbi.nlm.nih.gov/ tools/primer-blast/). All primers fulfilled the requirements described above.

Even if BLAST analysis of the primer pair shows that the primers should not give any unspecific amplification, the specificity of PCR product should be confirmed. First of all the PCR products should be separated by their weight by gel electrophoresis and match the expected weight corresponding to the sequences of the amplified areas. Another important step is sequencing of the PCR product. If there is only one band detected on the gel, the content of the tube from the PCR reaction can be sequenced. In case of multiple PCR products the DNA can be purified from the definite band on the gel, and the result of this purification can be sequenced. It is also possible to run so-called "nested PCR" where the tested PCR product is used as a template, and the primers are constructed to amplify the area within the PCR product. Nested PCR is an easy and quick way to test the specificity of the PCR product, but is limited by the size of it, as the template should be long enough for a new pair of primers to produce the products of detectable size. In the case of qPCR experiments the products are usually around 100-200 bp, so nested PCR is difficult. In this case the preferred method is to sequence the PCR product.

To study alternative splicing of Best3 mRNA in mouse tissues (Paper II, III and IV) we developed sets of primer pairs (see Supplement Fig.1S and Table 2 in Paper II, Table 1 in Paper III), in all these papers we used the same primers for mBest3. Alternative mRNA splicing in mouse tissues produces Best3 splice variants where exons 2, 3 and 6 can be absent in different combinations. We used primer pairs spanning the area with possible exon excision, and in the case of alternative splicing saw multiple PCR products as bands on the gel corresponding to predicted size of longer (heavier bands) or shorter (lighter bands) splice variants. To demonstrate the possible presence or absence of the exon we also used primer pairs where one of the primers was complementary to the area of the exon of interest. If the splice variant containing this exon was present in the sample, the PCR

product was detected as a band of expected weight. To confirm the efficiency of the primers we used mouse heart tissue known to express full-length Best3 mRNA as a positive control (62).

For qPCR quantification of the long "-2-3+6" splice variant expression in mouse tissues we used primers spanning exons 6 and 8. To detect the short "-2-3-6" splice variant we used a special forward primer with 5' half complementary to the 3' end of the exon 5, and with 3' half of the primer recognizing 5' end of exon 7. To quantify the total Best3 mRNA (all splice variants together) in the mouse we used the primer pairs spanning exons 9 and 10, as this area does not have alternative splice variants.

In the qPCR experiments in Paper II we sequenced the PCR products. We also tested the qPCR products on the gel (Fig.2 A) and estimated efficiency for our Best3 primer pairs (Fig.2 B). Primer efficiency was determined as the relation between PCR threshold cycle number and relative initial template concentration in a series of sequential two-fold dilutions of pooled cDNA. Efficiency was calculated as 2^(-1/slope)-1 and expressed as per cent.

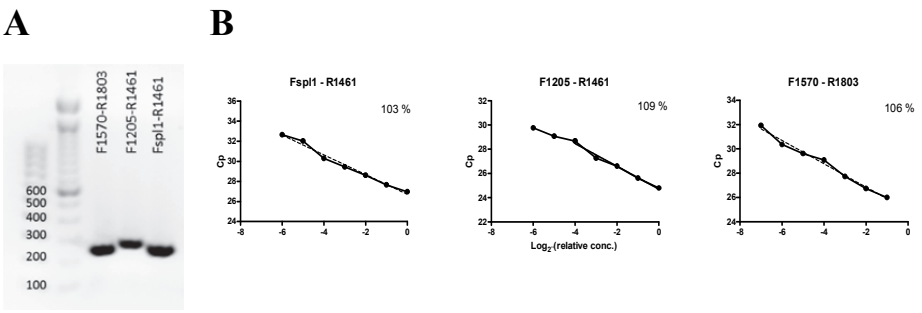

Fig.2 ***Control of specificity and efficiency of mBest3 primers used in our qPCR experiments****. Primer pairs were specific for detection of Best3 template as the qPCR products showed single bands of expected weight in gel electrophoresis (panel A), and sequencing of these qPCR products confirmed that the correct template was amplified. The primer pairs also showed good efficiency in the test experiments with serial dilutions of the template (Panel B).*

In Paper I we studied the expression of total mRNA for Best3 in the rat and used the pairs of primers localized in exons 6-7 and 9-10. All the qPCR products showed only one specific band with expected size. Some primer dimer detection was observed for most of mouse Best3

primer pairs, but their detection was seen later than the detection of Best3-specific product.

3.3.3 Protein structure analysis

On the basis of the mRNA sequence the amino acid sequence of the protein can be predicted. The real protein sequence can be detected by mass-spectrometry techniques, but the majority of information in protein databases for animals and humans is still based on predicted protein sequence and structure. Further from the amino acid sequence secondary structures and 3D-models of the protein can be predicted and analyzed. These *in-silico* studies were not among the major aims of this thesis, but as function and regulation of Best3 are unclear, this additional information can be useful.

For searching for similarities between the nucleotide or amino acid sequences we used a multiple sequence alignment program ClustalX 2.1. In Paper I for rat Best3 we predicted the transmembrane structure using TMHMM algorithm (Prediction of transmembrane helices in proteins, http://www.cbs.dtu.dk/services/TMHMM/) (46) and phosphorylation sites for protein kinase G using GPS 2.0 (Group-based Prediction System, http://gps.biocuckoo.org/index.php) (103). Later we did the same analysis for mouse full-length Best3 and for its short splice variants. We also made very preliminary analysis of protein structure of mouse Best3 splice variants using Phyre2 (Protein Homology/analogY Recognition Engine V 2.0) available on-line http://www.sbg.bio.ic.ac.uk/phyre2 (42).

3.4 Study of Best3 function

3.4.1 Electrophysiological studies in vascular smooth muscle: Patch-Clamp recording

Patch-clamp techniques allow studying the activity mostly of ion channels, but also of electrogenic transporters and pumps by recording electrical current through the cell membrane. This technique can be used in isolated cells and in some tissues. The main principle of patch-

clamp technique is that a low resistance glass pipette is sealed to the cell membrane and serves as a recording electrode, while the reference electrode is placed extracellularly. The membrane potential is fixed at a set level (voltage clamp), and the current in the patch pipette represents the current through single or multiple ion channels activated in response to the change of the membrane potential or intra- and extracellular environment.

In our experiments with cultured vascular smooth muscle cells (Paper I) we used a whole cell patch clamp technique. The patch pipette was sealed to the cell surface, and then the membrane area inside the pipette was removed to get a low-resistance access to the intracellular environment. In this case we controlled the intracellular environment by the solution in the pipette and recorded the currents across the whole membrane of the cell in response to changes in membrane potential or in extracellular solution.

To be able to see chloride currents we maximally excluded all the other ions, first of all sodium and potassium ions producing the biggest currents in the cell. Chloride concentrations were equilibrated inside and outside the cell, and cesium was used as a counter-ion for chloride, as it blocks the potassium channels and cannot travel across the membrane. In this case inward chloride flux was recorded as positive, and outward as negative current.

Niflumic acid was used to block the classical calcium-activated chloride currents and zinc ions to block the cGMP-dependent chloride current.

3.4.2 Suppression of protein expression in vascular smooth muscle by RNA interference

Transfection methods

One way to discover functions of a protein is to observe changes in the cell or tissue in the absence of the protein or when the expression of it is reduced. One possibility is to produce a gene-modified animal where the protein of interest is not produced because its gene cannot be expressed or translated. This can be achieved either on the level of the whole organism (global knockout) or in a definite cell type

(conditional knockout) through the whole life of the animal or starting from a definite time point (inducible knockout). Creating a knockout mouse is a very powerful tool, but it is a long, difficult and expensive process, and sometimes the animal can develop compensatory changes which can mask the function of the protein of interest. The intervention to the genome can also give side effects changing the expression of irrelevant genes. For Best3 there are no knockout models currently available for purchase. Instead we used a method to downregulate Best3 gene expression by RNA interference (Paper I). In this method the mRNA for the protein of interest is destroyed by interaction with a small interfering RNA (siRNA). siRNA is a short (20-25 bp) double-stranded RNA with a sequence complementary to the target mRNA of interest. siRNA binds the target mRNA and causes its degradation by interacting with RNAi induced silencing complex (RISC). The efficiency of siRNA-based downregulation depends on the level of gene expression, and the changes in mRNA level can be seen first. Downregulation of the protein usually comes later, and the effect on the protein expression depends on the turnover of the protein in the cell. This is why not only mRNA quantification, but also quantification of the protein of interest after siRNA transfection is necessary.

For genes known to have different variants of mRNA alternative splicing, RNA interference can be used to selective downregulate either one of the splice variants (if siRNA recognizes the area present only in the splice variant of interest) or all splice variants at once (if siRNA is complementary to the area which is present in all variants). In our experiments we used two different anti-Best3 siRNA, which were created complementary to the sequences in exon 7 and 10 in the rat Best3 gene. There is no data for alternative splicing of Best3 mRNA in the rat, but by analog comparison with the mouse Best3 mRNA, it is likely that both siRNAs that were used downregulated all splice variants of Best3.

siRNA transfection is more often used in cell culture because siRNA delivery can be difficult in the tissue. In our experiments we transfected cultured vascular smooth muscle cells with anti-Best3 siRNA, but we also developed an original method to transfect the mesenteric arteries in rats *in vivo*. To deliver siRNA to the cells we used a lipofection technique where siRNA is placed inside the liposomes, which being hydrophobic, can merge into the cell

membrane and deliver its content to the cytoplasm. This is a commonly used technique in cell culture experiments, but the penetration of the liposomes into tissue is difficult. We found that the optimal method to transfect the vessels *in vivo* was a combination of lipofection with magnetofection where magnetic forces created a dragging force, helping nucleic acids to enter the target cells. This procedure was performed in anesthetized animals, where a segment of the intact mesenteric artery was transfected in a small silicon bath on top of a magnet and then stayed in the animal for 3 days, until the animal was sacrificed. This method cannot be used for long-term chronic *in vivo* experiment, as siRNA will be degraded in the cells with time, so for long-term RNA interference experiments the method of short hairpin RNA (shRNA) would be more appropriate. In our experiments 3 days of siRNA exposure was sufficient to downregulate Best3 mRNA and protein in the vessel.

Except the slow penetration of siRNA into the tissue, there are other problems with tissue transfection compared to the cell culture experiments. Methods of transfection can be quite harmful for the tissue, and time for the tissue to recover can be longer than the effect of siRNA downregulation. Further, as all the cells present in the tissue get transfected, it is difficult to connect loss of function to a definite type of cells.

Control experiments for the siRNA-induced knock-down

In experiments with siRNA-based downregulation of function, proper control experiments are required.

- Control of efficiency of transfection: It is necessary to find the most efficient and harmless way to transfect the cells/tissues, first with a simple fluorescent dye, and then with fluorescent-labeled siRNA;
- Control of efficiency of knock-down of mRNA and protein: Quantification of mRNA with qPCR and of protein with WB should be done at different time points to find the maximal downregulation of protein of interest;
- Control of specificity of downregulation: Scrambled siRNA (nonsense siRNA not recognizing any target in the living species), mutated siRNA (siRNA against the target sequence containing few single nucleotide mutations), non-relevant siRNA (siRNA created

against the target gene which does not exist in the studied species, for example anti-GFP siRNA used in a mouse), two or more different siRNAs against the same mRNA target can be used;

- Control of side effects of the transfection procedure: Transfection with scrambled siRNA should not influence normal functioning of the cells/tissue.

3.4.3 Models of cell and tissue injury

ER stress (Paper II, III)

Endoplasmic reticulum (ER) stress in cells can be present in different kinds of injury, sometimes as a secondary response, for example, as a reaction to the inflammation induced by injury. When ER is the main interest of the study, it can be induced directly, for example, by heavy metal poisoning, by antibiotic tunicamycin causing misfolding of proteins by inhibiting N-linked glycosylation or by thapsigargin (TG) blocking the SERCA pump in the ER and exhausting ER from calcium. Most often such experiments are done in cell culture as these agents are quite poisonous. In our experiments we used TG treatment in cultured podocytes and astrocytes in concentrations of 200-500 nM, commonly used in such experiments.

LPS-induced inflammation (Paper II, III)

LPS (lipopolysaccharide) is a bacterial endotoxin, which is the major component of the cell wall of Gram-negative bacteria. *In vivo* it is present in blood as a result of bacterial infection, in smaller concentrations it causes a strong immune response and inflammation, and in high concentrations – septic shock. LPS-induced immune responses are mediated, among the other cell receptors, by Toll-like receptors 4 (TLR4), which are transmembrane receptors transmitting the signal from cell surface to the cytoplasm. Sepsis involves TLR4-independent cytoplasmic action of high doses of LPS (69; 92).

In experimental research LPS injections (i.p. or i.v.) are used to induce inflammation in animals. Commercially available LPS varies substantially in its purity and activity between providers and even between the batches purchased from the same company, which can be one of the reasons for the large range of concentrations of LPS used in cell cultures and *in vivo* experiments. In our experiments *in vivo* (Paper

II) we used 1mg/kg of body weight which is considered a low-dose LPS injection in rodents and should not induce acute renal failure in mice but will induce proteinuria similar to other proteinuria models (23; 74).

Neonatal hypoxic-ischemic brain injury (Paper III)

We performed hypoxia-ischemia (HI) according to the Rice-Vanucci model (75; 79) in nine-day old mice of either sex. In this model, as a result of combination of hypoxia and blood vessel ligation the cerebral blood flow (CBF) in the left hemisphere ipsilateral to the artery ligation is reduced transiently during the hypoxic exposure. HI-induced injury (Fig.3) develops in the left hemisphere, while no significant morphological changes are observed in the hypoxic right hemisphere (97). The right contralateral hemisphere experiences only hypoxia, and no fall in CBF is observed (29). In the studies in the thesis we used exposure to 10% of oxygen for 50 min, which resulted in brain injury predominantly in the hippocampus and cortex.

Fig.3 ***Coronal section of the mouse brain three days after HI****. Permanent unilateral occlusion of the common carotid artery was performed followed by exposure to hypoxic environment. In the ipsilateral hemisphere (left) the injured areas appear mostly in hippocampus and in the cortex. The contralateral (right) hemisphere is exposed only to hypoxia and does not have visible areas of injury. For visualizing the injury the brain tissue was stained with thionin/acid fuchsin.*

Using the HI model it is possible to separately study the effects of hypoxia only (right hemisphere in HI-exposed pups VS right hemisphere in sham-operated) and HI (left in HI VS left in sham). Changes during HI injury, but not associated with hypoxia alone, can be studied by comparing the right hypoxic hemisphere and left hypoxic-ischemic hemisphere of the same animal.

4 SUMMARY OF THE RESULTS

We showed that Best3 is essential for the calcium-activated cGMP-dependent chloride current described previously in rat vascular smooth muscle. In cultured rat aortic smooth muscle cells this CAC current co-existed with “classic” CAC current, but appeared only in the presence of cGMP, it was voltage-independent and had a linear current-voltage relation. It had low sensitivity to niflumic acid, but was instead highly sensitive to zinc and to inhibition of PKG activity. Best3-directed siRNA transfection of cultured aortic cells reduced Best3 mRNA level to about 20% and protein level to about 45%, but totally eliminated cGMP-dependent CAC current. Expression of Best1 and 2 mRNA was unaltered, and the classical niflumic acid-sensitive CAC current was not changed. Similar results were obtained in experiments with in-vivo siRNA-based silencing of Best3 in rat mesenteric arteries. (Paper I)

In the mouse Best3 protein was detected by immunohistochemical methods in kidney (Paper II), neonatal brain in normal conditions and after HI injury (Paper III), intestine (Paper IV). Best3 staining was seen mostly intracellularly, except in kidney vasculature and in brain ependymal cells, where the staining seemed to be associated with cell membrane.

In mouse kidney immunochistochemical analysis detected Best3 in podocyte cell bodies and primary processes, but not in the foot processes, where it co-localized with the intermediate filament nestin. Immunogold-based electron microscopy experiments in kidney tissue confirmed intracellular localization of Best3 protein in podocyte cell bodies and primary processes. Immortalized cultured podocytes also showed Best3-positive staining which had similar pattern with the ER marker calnexin and the mitochondrion marker ATP5F1, but Best3 staining did not fully overlap with these proteins. Best3 could also be seen in the vasculature in kidney specimens, mostly in smooth muscle cells, but probably also in endothelial cells in the bigger vessels (Fig.4).

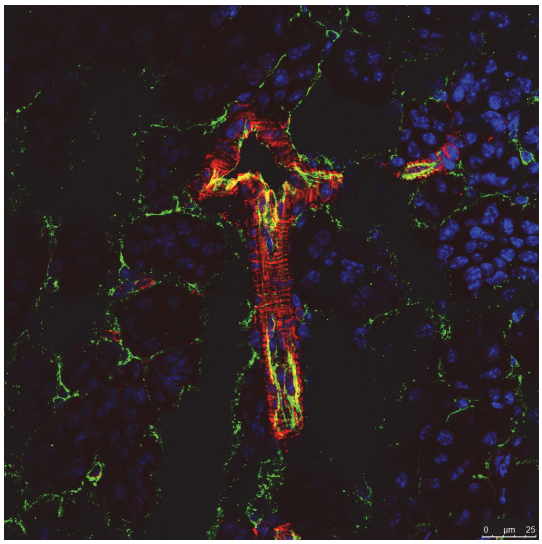

Fig.4 ***Immunofluorescent detection of Best3 protein in the vasculature in mouse kidney*** *(frozen samples). Best3 (red) can be seen in smooth muscle cells in the wall of the blood vessel. The borders between the vascular smooth muscle cells can be clearly seen which suggests that the staining can be localized in the cell membranes. Best3 seems to partially co-localize with endothelia marker CD31 (green) in the big vessel, but not in the small vessels.*

In newborn mouse brain Best3 protein was detected in ependymal cells of the brain ventricles (Paper III). Our preliminary data in adult healthy mouse brain also detected Best3 in brain ependymal cells (Fig.5 A). After HI injury in newborn mouse brain Best3 was detected also in a subpopulation of nestin-expressing astrocytes, but only in the injured hemisphere (Paper III). Already 24 hours after injury the Best3-positive structures were observed in some perivascular areas in the core region of the injury (Fig.5 B), but strong expression of Best3 in astrocytes was observed 72 hours after injury. Astrocytes with the strongest expression of Best3 appeared to have lower expression of GFAP. In primary culture of mouse astrocytes most of the cells were positive for Best3 and nestin.

In mouse intestine the expression of Best3 protein was detected in glia of myenteric plexus, in goblet cells and non-epithelial mucosal cells.

Our analysis of Best3 mRNA expression in mouse kidney, brain and intestine could not detect full-length mRNA, but showed in all these tissues the presence of the shorter variants of Best3 mRNA as a result of alternative splicing. In most of the tissues exons 2 and 3 were always absent, and exon 6 could be present (“-2-3+6” variant) or absent (“-2-3-6” variant). In intestine, in a sample of smooth muscle

also containing the enteric nerves, we detected a very low amount of Best3 splice variant containing exon 3. This splice variant was not studied further, as exon 3 in mouse Best3 does not contain any starting codon for protein translation, and on the level of protein this splice variant will not be different from the other variants lacking both exon 2 and 3.

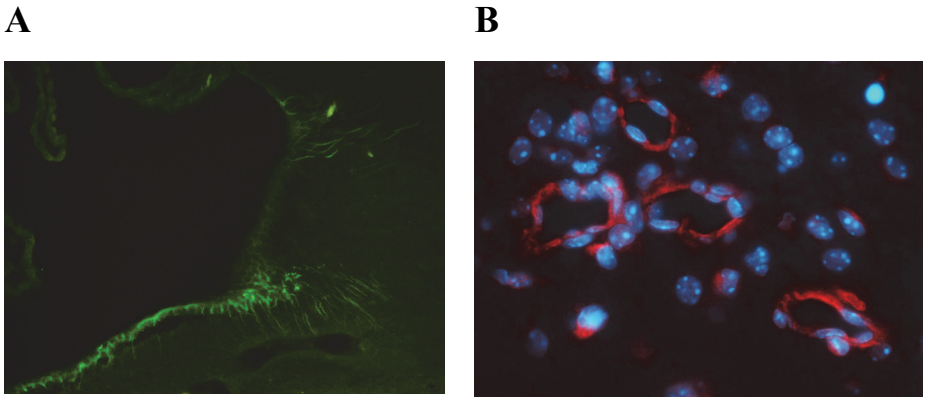

Fig.5 ***Immunofluorescent detection of Best3 in mouse brain****. In normal conditions Best3 protein can be detected in the brain in ventricular ependymal cells of the adult (panel A, green) or newborn (Paper III) mice. The staining suggests probable localization of Best3 in association with the cell membranes.*

In the injured brain of neonatal mice (HI model) Best3 was detected in astrocytes in the core and penumbra-like areas of the injury. The maximal intensity of the staining was observed three days after HI (Paper III), but could also be seen at 24-48 hours after HI (panel B, red) when the staining very often was observed in association with brain vasculature. No Best3 was detected in astrocytes in the healthy brain of sham-operated mice or in hypoxia-exposed contralateral brain hemisphere of the mice after HI. Blue staining with DAPI in panel B visualizes cell nuclei.

In our experiments with tissue injury (Paper II and III) the presence of ER stress was detected as an increase in mRNA expression of the ER-stress marker CHOP. Thapsigargin (TG) was used in podocyte and astrocyte cell cultures to induce ER stress through blocking of the SERCA pump, which caused a pronounced increase in expression of CHOP in both types of cells. We also observed signs of ER stress in kidney glomeruli after LPS treatment (but not in LPS-treated podocytes) and in in the HI-injured brain hemisphere (but not after hypoxia alone). LPS treatment did not increase CHOP expression in

cultured podocytes. In astrocytes LPS induced a small increase in CHOP, and in the case of pretreatment with LPS before TG an additive effect on CHOP expression was seen.

Best3 mRNA expression was changed in LPS-treated kidney glomeruli, after hypoxia and hypoxia-ischemia in the brain, and also in TG-treated podocytes and astrocytes. Changes in expression of Best3 splice variants "-2-3+6" and "-2-3-6" showed different patterns in different models of injury (Fig.6 A). Both splice variants changed in the same direction (upregulated) after TG treatment in podocytes and astrocytes, in response to hypoxia and in the case of later response to LPS in glomeruli. During the early response to LPS in glomeruli only the "-2-3+6" splice variant was upregulated. Hypoxic-ischemic brain injury caused opposite changes in expression of Best3 splice variants: the "-2-3-6" variant was upregulated, while the expression of the "-2-3+6" variant was decreased.

Analysis of the expression of Best3 splice variants as the ratio "-2-3+6"/" -2-3-6" showed that in different tissues the proportion of splice variants was different (Fig.6 B, Paper IV). The "-2-3-6" variant was prevailing in glomeruli, kidney, in cultured mouse astrocytes and in the brain at early time points after HI injury. The "-2-3+6" variant was expressed more in the healthy brain and in the brain exposed to hypoxia, in the brain at later stages after HI, in cultured podocytes and in the muscle+enteric nerve fraction of the intestinal wall. In intestinal epithelium "-2-3+6" and "-2-3-6" variants were expressed almost equally with a slight prevalence of "-2-3+6" variant.

Together with Best3 mRNA expression and splicing, we also studied the expression of intermediate filament nestin. In both models of the tissue injury nestin expression always changed in the same direction as CHOP. The time course of changes in nestin and CHOP expression was also similar, except in HI-induced brain injury, where overexpression of nestin developed more slowly than the increase in CHOP.

Pretreatment of astrocyte culture with LPS prevented TG-induced increase in expression of nestin, and also reduced the TG-induced changes in expression of both Best3 splice variants.

A

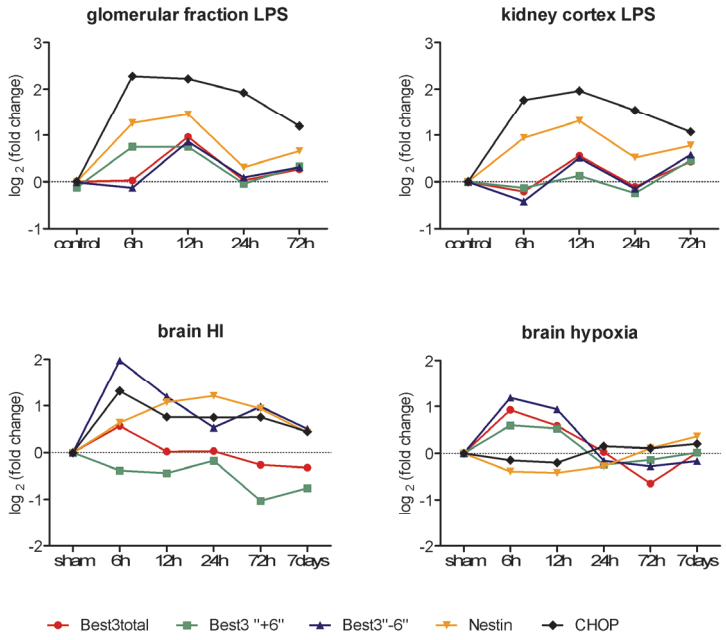

B

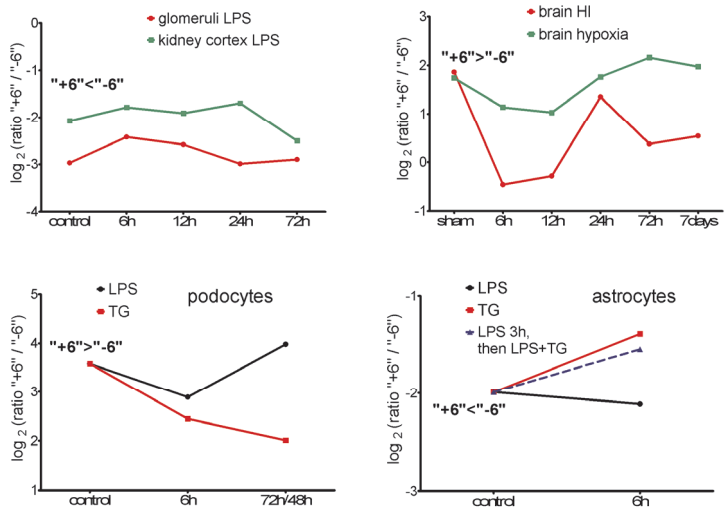

Fig.6 ***Expression of mRNA for Best3, intermediate filament nestin and ER-stress marker CHOP in mouse tissues and cells before and after injury****. Panel A: ER*

stress was present in the kidney and glomeruli after LPS treatment and in the brain after HI, but not in the brain after hypoxia only. Analysis of the changes only in total Best3 mRNA was not sufficient, as Best3 splice variants were responding to the injury differently. They were changing either with different time course ("-2-3+6" variant got upregulated in glomeruli earlier after LPS treatment) or their expression level was changing in different direction (in brain after HI "-2-3+6" variant was downregulated, and "-2-3-6" variant was upregulated). Panel B: The ratio between splice variants of Best3 mRNA was different between different tissues and different cell types. In control conditions the long "-2-3+6" variant was prevailing in brain and in podocytes, and the short variant "-2-3-6" was dominant in kidney cortex, glomeruli and astrocytes. The figure represents only the changes in the mean values for the groups, the individual data distribution and statistical analysis of the changes can be found in the Paper II and III.

The response of Best3 splice variants after injury in both kidney and brain tissues always had a biphasic pattern (Fig.6 A): at early time points the levels of expression of both splice variants were changed, but at 24 hours they were recovering and close to control values, and at later time points the values were changing again. The same tendency was observed for total expression of Best3 mRNA.

5 DISCUSSION

The main interest of this work is directed to the localization and function of Best3, a protein with multiple functions, in different tissues in rodents.

5.1 Best3 as a calcium-activated chloride channel in vascular smooth muscle

Calcium-activated cGMP-dependent chloride current participates in synchronization in vascular wall

The history of this project started from the investigation of regulation of blood vessel tone, in particular the mechanisms of vasomotion – spontaneous fluctuations in vascular tone, observed in resistance vessels in many vascular beds in animals and humans. The function of these spontaneous fluctuations is not clear, but their disturbance is often associated with cardiovascular dysregulation, for example in diabetes and hypertension. In the 1990's and early 2000 Nilsson and coworkers performed studies in rat mesenteric arteries and developed a hypothesis of generation of vasomotion (1; 35; 36; 61; 66). According to this hypothesis, there are no definite oscillators in the vascular wall, but the sarcoplasmic reticulum of each vascular smooth muscle cell (VSMC) plays a role of oscillator, so in each VSMC spontaneous increases in intracellular concentrations of calcium (so-called calcium waves) can be observed in the presence of a vasoconstrictor. In these arteries, the activity of these oscillators is not synchronized between different cells until a critical moment when all calcium concentrations in VSMC start oscillating in phase. At the same time synchronized changes in membrane potential of VSMCs emerge, and this results in synchronized oscillations in vascular tone, so called vasomotion. In the absence of intact function of endothelium the synchronization of VSMC oscillators and appearance of vasomotion was not possible, even if calcium waves in VSMC were still present. In the absence of the endothelium, application of membrane-permeable cGMP caused reappearance of oscillations, showing that the oscillations are generated in the smooth muscle, and cGMP has a permissive role (35; 36).

The question what triggers the synchronization of VSMC oscillators remained until it was discovered that the release of calcium from intracellular stores induces a depolarizing inward current in VSMC, which can cause the change in membrane potential. This current was dependent on the presence of cGMP – the intracellular messenger appearing in VSMC in response to endothelium-derived nitric oxide, which explains the importance of intact endothelium for vasomotion. The search of possible candidates for this "synchronizing" current led to the discovery of a novel cGMP-dependent calcium-activated chloride (CAC) current in VSMC. This current differed from "classical" CAC currents by electrophysiological characteristics, had low sensitivity to "classical" CAC channel blockers such as niflumic acid, but instead could be blocked by zinc (55), so it was suggested that the molecular identity of this channel is different from the already described CAC channels. At the same time novel putative CAC channels, bestrophins, had just been described. Bestrophins were shown to be CAC channels (73; 89), and the characteristics of bestrophin-associated CAC current were very similar to that of the cGMP-activated current in VSMC suggesting that it may be of bestrophin origin. Paper I is dedicated to revealing the identity of the cGMP-dependent CAC channel in VSMC (either in cells freshly isolated from rat mesenteric arteries or in a cell line of rat aortic smooth muscle cells).

Best3 is a candidate for calcium-activated cGMP-dependent chloride current in rat vascular smooth muscle cells

In cultured rat VSMC, which have a pronounced cGMP-dependent CAC current, the qPCR analysis of the mRNA expression showed that the Best3 isoform is expressed in these cells to a greater extent than the other isoforms (Best1 and 2). The appearance of a cGMP-dependent CAC current in VSMC from different vascular beds was accompanied by expression of Best3 mRNA and protein (detected by WB). These data brought the Best3 isoform in focus of further investigation. Downregulation of Best3 by siRNA technique in cultured VSMC caused disappearance of the cGMP-dependent CAC current, even if the Best3 protein level was reduced to only about 45%. There is no obvious explanation for this, but it is possible that Best3 can be present in the cell in different splice variants or be localized in different cell compartments, and these different fractions of proteins might have

different turnover and life-time, so the ion channel fraction can be downregulated earlier than the others. In our experiments in cultured VSMC downregulation of Best3 did not cause change in expression of Best1 and 2 mRNA. In later work of Dam and others (Dam V., PhD thesis, Aarhus University, 2014) siRNA-based silencing of Best3 caused downregulation of mRNA also of other bestrophins. The reason for this discrepancy is not clear, but in their work the transfection was performed *in vivo*, and analysis of mRNA expression was made on homogenate of the whole vessel. Based on the results in A7R5 cells it is clear that Best3, but not Best1 or 2, is associated with the cGMP-dependent CAC current. However, the question if Best3 itself forms a channel or if it is a regulator of other CAC channels remains unanswered. There is data of Dam and others (24) that siRNA-silencing of anoctamin-1 causes downregulation of the "classical" current, but also of Best3 mRNA and the cGMP-dependent current. This work was also performed with *in vivo* transfection and the mRNA analysis represents changes in all types of cells in the vascular wall. The disappearance of cGMP-dependent current in this situation suggests that Best3 might be a regulator of the anoctamin-1 channel.

From our data we can see that cGMP sensitivity of the Best3-related current is associated with activity of PKG. There is the possibility that PKG directly phosphorylates rBest3, as a few PKG-phosphorylation sites can be predicted in rBest3 (Paper I, Supplement) and in mBest3 (Fig.7). The Best3 isoform was previously shown to have an autoinhibitory effect on the channel activity by its C-terminus (73). Phosphorylation might cause conformational changes of the C-terminal part of the protein which can break the autoinhibitory protein-protein binding and activate the Best3 channel or another CAC channel, if Best3 is a channel regulator. The possibility of bestrophins to be phosphorylated has previously been proposed (28; 53), but the suggestion that PKG-induced phosphorylation can be involved is discussed for the first time in our paper. Removal of the autoinhibition by phosphorylation could involve detachment of the C-terminus from membrane phospholipids (71), mechanical opening of the channel, or revealing the calcium-sensing area of protein. On the other hand, PKG may affect Best3 indirectly, through activation of other intracellular pathways.

The identification of Best3 as a CAC channel in vascular smooth muscle cells is a novel and important discovery and suggests that Best3 can perform channel functions not only in experiments with overexpression in cell culture, but also *in vivo*. Until now there was only one other such demonstration: Best3 was shown to be a CAC channel in mouse cardiomyocytes (62). But in this paper the Best3-associated CAC channel was active and did not require activation by cGMP, while in rat smooth muscle it was strongly cGMP-dependent. This difference could be explained by different species used in the experiments of O'Driscoll and our group: mBest3 can undergo alternative splicing, while there is no evidence for this for rBest3. The other possible explanation could be that the endogenous levels of cGMP or endogenous activity of PKG in mouse cardiomyocytes are higher than in rat VSMC. Best3, functioning as a CAC channel, is an important player in generation of vasomotion in vasculature (14). As Best3 was suggested to participate in synchronization of calcium oscillations between cells, it might be involved in a similar way in e.g. cardiac pathology, as calcium oscillations were reported to participate in reperfusion-induced injury in rat cardiomyocytes (2).

5.2 Localization and function of Best3 in mouse tissues

In our further studies (Papers II, III and IV) we investigated the expression and function of Best3 in tissues other than vascular smooth muscle. Our previous experiments were done in rat, but we decided in the further studies to use mouse models to study Best3 localization and function, as the mouse genome and protein structure are more studied than those of rats, and also the possibility of using gene-modified mouse models was attractive. The knock-out model for Best1 is described in the literature (52; 54), but there are no knock-out models for Best3 described or commercially available so far.

Immunohistochemical detection and cellular localization of Best3 protein (Paper II, III and IV)

By immunohistochemical methods we discovered expression of mBest3 in kidney podocytes and in the epithelium of proximal tubules (Paper II), in brain ependymocytes and astrocytes after injury (Paper

III), and also in intestinal glia of myenteric plexus and in epithelial goblet cells (Paper IV). We also observed staining in blood vessels in the mouse tissues. In ependymal cells, in proximal tubule epithelium and in smooth muscle cells of blood vessel Best3 seemed to have cell membrane-associated localization, but, having only confocal images, it was not possible to determine if the protein was localized within the membrane or intracellularly close to the membrane. Intracellular localization close to the cell membrane was reported for Best1 in porcine RPE cells by Strauss and others (87). At the same time Best3 staining in mouse cardiomyocytes showed membrane localization (62). In goblet cells we found staining localized in the periphery of the cell. As these cells are expanded by mucin-containing vesicle, Best3 could be localized in the thin layer of cytoplasm squeezed along the membrane, rather than directly associated with the membrane. In intestinal glia Best3 also appeared to be localized intracellularly. In podocytes and astrocytes Best3 showed clear intracellular localization in tissue as well as in cultured cells.

In tissue podocytes Best3 did not co-localize with a marker for foot processes, but was highly expressed in cell bodies and in primary processes where it co-localized with the intermediate filament nestin. Electron microscopy (EM) experiments confirmed the intracellular localization of mBest3 in podocyte cell bodies and primary processes. No staining was seen in foot processes and no Best3 was observed in the cell membrane or in close vicinity of it.

Best3 protein is co-localized with nestin in kidney podocytes and in brain astrocytes (Paper II and III)

Co-localization of Best3 protein with the intermediate filament, nestin, in podocytes and astrocytes after injury is an important discovery in the present thesis. Nestin is a commonly used marker for progenitor cells in the nervous system and also for tumors, it is expressed in some brain cells after brain injury (41) as well as in vascular smooth muscle undergoing remodeling (64).

In healthy kidney nestin is highly expressed in podocytes in mouse (98) and human (10; 88) and is suggested to have a protective role against podocyte injury. It is down-regulated in some types of kidney dysfunction where podocyte apoptosis is present, such as IgA nephropathy with proteinuria, membranous nephropathy and focal

segmental glomerular sclerosis (88). In puromycin aminonucleoside (PAN)-induced nephritis, where podocyte apoptosis is not seen, nestin is overexpressed (99). The severity of albuminuria in diabetic nephropathy was inversely related to the level of nestin expression (51), and in mouse cultured podocytes high-glucose-induced apoptosis was increased by siRNA-induced knock-down of nestin (50). Co-localization of Best3 with nestin might support the notion that Best3 is involved in podocyte protection.

In the brain under normal conditions nestin is typically expressed in cells of progenitor type, but after injury it starts to be expressed in activated astrocytes (33), probably in cells at an early stage of activation (22) that are able to proliferate and have a positive influence on tissue recovery (90). In neonatal brain after HI injury nestin-positive cells were suggested to be in transition from radial glia to astrocytes (82). Astrocytes positive for Best3 were typically nestin-positive. Best3-positive cells also express GFAP, but Best3 expression seems to be stronger in cells with a lower expression of GFAP. These Best3-positive cells can be newly-formed astrocytes, as GFAP is expressed in mature astrocytes.

Our staining for Best3 in mouse intestinal wall has a pattern very similar to the staining for nestin in rat intestine published by Cantarero Carmona and others (18), where the authors detected nestin in GFAP-positive glia-like cells of myenteric plexus. It seems that expression of Best3 in mouse is associated with a glial type of cell positive to nestin and GFAP. Even podocytes were shown to express the glial marker GFAP (15) and were discussed as cells sharing similarities with brain astrocytes (16). More research is required to explain why Best3 in mouse tissues can be expressed in two very different kinds of cells: either together with nestin in cells of glial type and in podocytes or in different cells of epithelial type typically not expressing nestin (e.g. intestinal goblet cells and brain ependyma of the brain ventricles). It will be interesting to understand the relation between Best3 and intermediate filaments (nestin, GFAP) and to see if the connection between Best3 and nestin is functional.

Subcellular localization of Best3 protein in podocytes: possible association with endoplasmic reticulum (Paper II)

As we used an antigen-retrieval procedure and cryostat sectioning, the resolution in the EM images did not allow us to detect in which cell compartment Best3 was localized. In immunofluorescence-based confocal images of cultured podocytes Best3 sometimes could be visualized in the periphery of the cells in membrane folds looking like cell attachment points. However, most of the staining was always localized in the center of the cell, mostly in the perinuclear area. There Best3 showed partial overlap with the ER-membrane protein calnexin and the mitochondrial marker ATP5F1 (the extramembraneous catalytic core of ATP synthase subunit), but did not show full co-localization with these proteins. The data strongly suggest that Best3 is localized in association with ER in podocytes, but more experiments with co-localization and EM techniques are required to confirm this. The possibility for bestrophins to be localized in ER was shown for hBest1, where it may serve as a counter-ion channel for other ion channels in the ER membrane (8).

It seems likely that in mouse podocytes mBest3 is associated with ER and may participate in ER function, while it is less likely that Best3 in mouse acts as an ion channel. In mouse tissues Best3 mRNA undergoes alternative splicing, and full-length mRNA has so far only been detected in cardiomyocytes (45; 62; 85). In the mouse tissues studied in our experiments (kidney, brain, intestine) we observed only spliced mRNA variants, so only truncated mBest3 proteins can be produced. Such proteins lack the pore-forming region and a transmembrane part as a result of excision of exons 2 and 3 ("-2-3+6") and sometimes also of exon 6 ("-2-3-6"). Thus these variants of mBest3 have likely lost the channel function, but they can still be associated with membranous structures as some of the hydrophobic areas are still present in the protein, and even the shortest "-2-3-6" variant of mBest3 can target the plasma membrane (85). Moreover, part of the mBest3 C-terminus, which is not known to be spliced, can also help to attach Best3 to the membrane by interacting with membrane phospholipids (71). Thus even intracellularly localized Best3, full or spliced, which has an intact C-terminus, can potentially associate with membranous cell compartments, such as ER.

The other observation pointing to a possible connection between Best3 and ER is that expression of Best3 mRNA changes during ER stress. ER stress develops when calcium starts leaking from the ER, which can cause mitochondrial injury, caspase activation and cell apoptosis. ER stress is also called unfolded-protein response (UPR) because it is characterized by accumulation of misfolded proteins in the ER. As a reaction to ER stress total protein synthesis levels fall to decrease the protein load of ER, while proteins directly participating in ER stress response become upregulated. ER stress can be caused by endogenous factors, e.g. free radicals or iNOS-derived nitric oxide. Under experimental conditions ER stress can be induced by a direct action on ER by calcium ionophores, SERCA blockers, and heavy metals, but also by LPS which might influence ER indirectly, by triggering inflammatory pathways in the cell (102). Previously it was shown in rat renal epithelial cells that Best3 expression plays a cell-protective role and its expression increases in response to ER stress induced by the SERCA blocker thapsigargin (TG) (49). Best3 was also shown to protect basilar artery smooth muscle cells from H_2O_2-induced injury (39). The authors did not discuss ER stress involvement but claimed that protective effects of Best3 are mitochondria-dependent, which may indicate ER stress induced by H_2O_2-related free-radicals. Other evidence of a protective action of Best3 is its role in inhibition of TNFα-induced NFκB-activation in endothelial cells (83). This may also be related to ER stress, as UPR and NFκB pathways can be connected (70).

Expression of Best3 mRNA changes after ER stress-related injury (Paper II and III)

In our experiments we saw changes in Best3 expression in two different kinds of tissue injury: LPS-induced kidney injury in adult mice (Paper II) and hypoxic-ischemic (HI) injury in the brain of neonatal mice (Paper III). In kidney we used low-dose LPS treatment as a proteinuria model (23; 74) that is associated with ER stress and elevation of CHOP (C/EBP homologous protein) (30). Mouse kidney and cultured podocytes express TLR4 receptors responsible for the specific LPS-induced inflammation (7; 69; 74). There is no other data on Best3 expression in LPS-induced inflammation, but Best1 expression was shown to increase in mouse kidney after LPS treatment (4). To induce brain injury in neonatal pups, we used a model of unilateral transient cerebral hypoxia-ischemia with reperfusion (75;

79). ER stress has been observed in brain injury models, for example following ischemia/reperfusion in adult rats (96), in neonatal HI injury (20) and in primary culture of rat astrocytes treated with oxygen/glucose deprivation, a cell culture analog of brain ischemia (9). There is no previous data on expression of any of the bestrophins in brain injury, but it was shown that Best1 protein is upregulated in the cell membrane and is responsible for CAC current in axotomized mouse sensory neurons, a model of peripheral nerve injury (12).

Thus in both tissue injury models used in our experiments ER stress is expected to be involved, and in both cases we saw upregulation of the apoptotic ER-stress marker CHOP and upregulation of total Best3 mRNA. Direct induction of ER stress by blocking the SERCA pump with TG in cultured podocytes and astrocytes had similar effects. Interestingly, we did not succeed to induce ER stress by LPS in cultured podocytes: neither CHOP nor Best3 expression was increased, which is in contrast to the induction of CHOP expression by LPS observed by Esposito and coauthors (30). Most likely this inconsistency is due to the methodological difference: we used an immortalized cell line of cultured mouse podocytes, while Esposito and coauthors used non-immortalized mouse podocytes. TLR4 receptors are expressed in podocytes in culture, however, the expression of other proteins participating in ER stress responses to LPS might be missing as a result of immortalization.

The fact that total Best3 expression often changes together with CHOP is an interesting observation in itself. The ER-stress marker CHOP, also called GADD153 or DDIT3, is a transcription factor known to induce cell cycle arrest and/or apoptosis in ER stress (65; 102). The mechanisms of its pro-apoptotic action are not fully understood. As a transcription factor it can induce the transcription of stress-related genes: it was suggested to downregulate Bcl-2 expression and to induce Bax translocation from the cytosol to the mitochondria (65). ER stress-associated CHOP activity is present in diseases such as diabetes, neurodegeneration and ischemia-related conditions (65) and is considered to be a sign of a pro-apoptotic state of the cells, but it is not clear if CHOP expression itself is always pro-apoptotic. The level of CHOP expression correlated with the degree of cell injury in astrocyte culture after oxygen/glucose deprivation, but only if CHOP was expressed constantly, not transiently (9). Further,

siRNA-silencing of CHOP had a protective effect, while overexpression of CHOP increased cell death (9). On the other hand, in kidney injury CHOP expression is necessary for cell survival as CHOP-deficient mice had more pronounced kidney injury and stronger inflammation after LPS treatment (30). In the epithelium of renal proximal tubules a protective effect of Best3 is due to the suppression of CHOP (49). If increased Best3 that we observed in glomeruli after LPS treatment, has a similar protective effect in podocyte injury needs to be studied more.

We found a complex relation between CHOP and Best3 expression in the experiments with HI in neonatal mouse brain (Paper III). When brain tissue experienced only hypoxia (the contralateral hemisphere of the brains from HI-exposed mice), the expression of Best3 mRNA increased, but at the same time the expression of CHOP mRNA did not increase, but rather showed a slight downregulation. Interestingly, nestin expression followed the pattern of CHOP expression in the hypoxic hemisphere. In the HI model used in this thesis, the hypoxic exposure to the contralateral hemisphere does not cause morphological signs of injury and cell apoptosis. This may explain why CHOP, usually associated with activation of apoptotic pathways, was not upregulated in contralateral hemisphere. Best3 upregulation was associated with downregulation of CHOP (49), so we speculate that hypoxia-induced Best3 upregulation in the brain prevents increase in CHOP and thus protects brain cells from injury.

Expression of two splice variants of Best3 mRNA in mouse tissues can be regulated differently after the injury

The understanding of Best3 expression in mouse tissues after injury is complex as there is extensive alternative splicing of mBest3 mRNA. Our data and data of others (45; 85) show that in mouse kidney and brain two splice variants are present, “-2-3+6” and “-2-3-6”. In order to investigate the different variants of mBest3 mRNA we analyzed by qPCR the total expression of mBest3 by amplifying the area in the mRNA corresponding to the C-terminus of the protein, which does not undergo splicing in mice. We also used pairs of primers specifically amplifying each of the splice variants separately. The results were quite intriguing: the ratio between “-2-3-6” and “-2-3+6” variants was different in different tissues and cells in control conditions (Fig.6 B),

the expression of the splice variants could be changing differently after injury, and even if total mBest3 expression was unchanged, we still could see a difference in the expression of the splice variants.

In glomeruli the shortest "-2-3-6" splice variant was prevailing under control conditions. Both splice variants were upregulated after the injury, however, the time course of these changes was different: the longer variant was upregulated at an earlier time than the short one. In cultured podocytes, on the other hand, the longer "-2-3+6" variant was dominant in control cells, but after the TG-induced injury the relative amount of the short variant increased. The difference between the responses of podocytes in the culture and in the tissue is likely due to the artificial milieu that the cells experience in culture. Podocytes in culture lack native three-dimensional cell architecture, properly formed cell-to-cell contacts and the regulatory influences from the neighboring glomerular cells, such as mesangial and endothelial cells.

In the brain tissue in control naïve animals the longer "-2-3+6" variant was the dominant form of Best3 mRNA, while in cultured astrocytes the short "-2-3-6" variant dominated. There were marked changes in the expression of splice variants in the brain after HI injury: the expression of the long splice variant was reduced, and the short splice variant was strongly upregulated. Thus, at the early time points after the injury the ratio between splice variants became opposite to the control values, and the expression of the short variant was most prominent. Astrocytes become activated in the tissue after injury, and they might be constitutively activated in primary culture from being stressed by the artificial conditions. This may explain why we saw a high level of Best3 protein expression in non-injured cultured astrocytes, while in the brain *in vivo*, Best3 protein was not detected in astrocytes until the injury had occurred. This can also explain why astrocytes in culture responded differently to the injury compared to the tissue cells: while the short variant was very little upregulated, the long variant actually increased its expression. Also in the situation of HI in the brain tissue astrocytes might not be directly injured, but more responding by activation to the pronounced injury in the neurons. In the cell culture experiments we induce injury in astrocytes themselves, which can cause a different response in astrocytes in culture compared to the *in vivo* experiments.

The opposite change in the expression of the longer and the shorter mBest3 splice variants after HI injury together with the data on Best3 cell-protective effects are reminiscent of the well-described injury-induced changes in the proteins of Bcl2 family, and in particular the member of this family Bcl2L1 (also called BclX). BclX mRNA can undergo alternative splicing, and the splice variants of BclX protein have different functions: the long Bcl-xL variant is anti-apoptotic while the short Bcl-xS variant is pro-apoptotic. In HI neonatal brain injury the ratio between Bcl-xL and Bcl-xS change. This is suggested to have a functional meaning, as selective downregulation of Bcl-xS by shRNA reduces brain sensitivity to HI (3; 100). The Bcl-xL variant of BclX as well as the Bcl2 protein are also expressed in mouse podocytes and change their expression in cyclin-I-null mouse podocytes that are sensitive to apoptotic stimuli (13).

Thus, analysis of the total change in mRNA for proteins existing in different splice variants, such as Best3, does not provide the full information about the gene expression. Different splice variants of the protein can have different functions, and their expression can be regulated differently on the level of mRNA by alternative splicing. Almost all the published data on Best3 expression is done without taking into consideration the alternative splicing of mRNA for Best3, and no analysis of expression of mBest3 splice variants in injury has previously been performed.

5.3 Relevance of the studies of Best3 alternative splicing in rodent models to human research

Predicted structure of Best3 protein is similar in mouse and human

The predicted structures of the full-length hBest3 and mBest3 proteins and predicted structure of the mBest3 splice variants (based on hBest1 model (37) and our analysis) are presented in Fig.7, for the model of rBest3 see Paper I, Supplement. The structure of the full-length mRNA transcript (the length of mRNA and the length of the protein product, the number and length of the exons) is very similar

between hBest3 and mBest3. Both consist of 10 exons, with exon 10 being the longest of all (Fig.1; 7). The first translational start-codon is placed in exon 2, and the next alternative start codon is localized in exon 4.

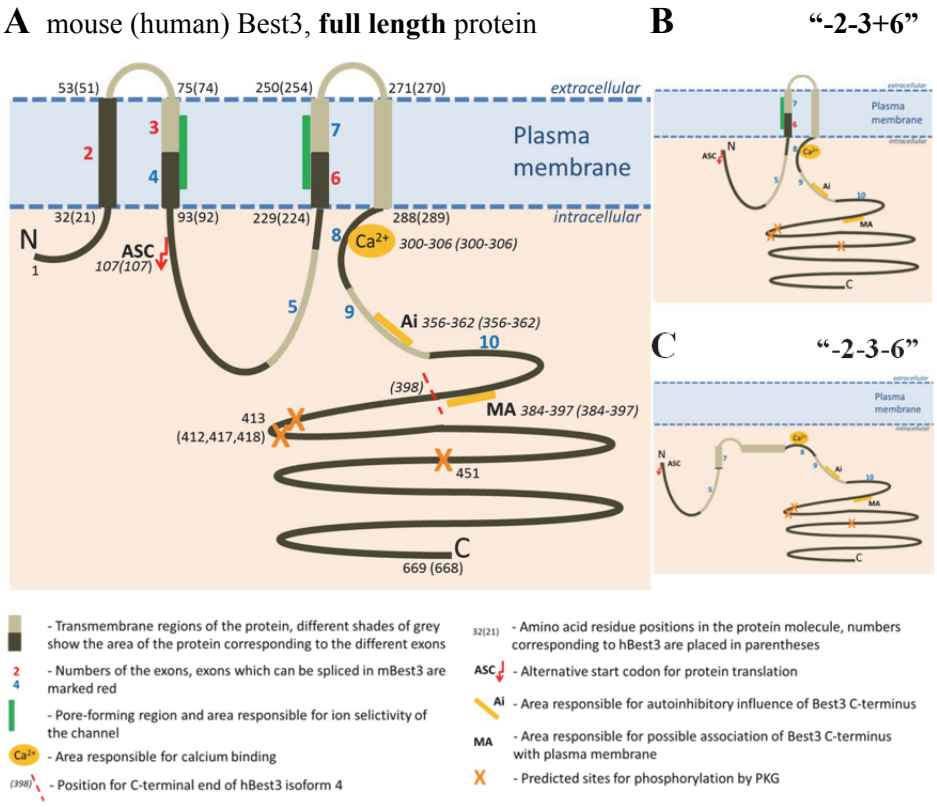

Fig.7 Predicted structure of Best3 protein for mouse and human*. The full-length Best3 (A) forms four hydrophobic transmembrane domains participating in formation of the channel pore. N- and C-terminal parts are located intracellularly. The protein-encoding region consists of nine exons, the first start codon for translation is localized in exon 2, and the alternative start codon lays in exon 4. The intracellular C-terminus contains areas responsible for calcium binding, for autoinhibitory function, for possible association with plasma membrane and also predicted sites of phosphorylation by PKG. The exon structure and the predicted protein structure are very similar between mouse and human Best3, and the positions of regulatory sequences are mostly the same (presented in the figure as amino acid residue positions for mouse and in parentheses for human). Predicted structures for splice variants of mBest3 protein, studied in our experiments, are shown on panel B and C. The "-2-3+6" splice variant (B) is predicted to be a transmembrane protein,*

while the "-2-3-6" variant does not seem to go through the membrane, but as it still keeps part of hydrophobic area, some kind of association of this splice variant with membranous structures might still be possible. For human mRNA we can find in databases the splice variant analogous to the mouse "-2-3+6", but also the variant where the major part of C-terminus is spliced out, so the corresponding protein will be lacking the regulation by PKG phosphorylation.

Alternative splicing of Best3 mRNA is likely to exist in both mouse and human

Alternative splicing for Best3 mRNA was previously studied in detail mostly in mice, where exons 2, 3 and 6 can be excised. For human Best3 alternative splicing of mRNA was reported in one publication (86), and six variants of hBest3 mRNA producing five splice variants of corresponding predicted proteins can be found so far in the NCBI Gene database (http://www.ncbi.nlm.nih.gov/gene/144453). However, analysis of existence and functioning of such protein products is lacking in the literature. The human variants most relevant to what we have seen in mice are the 1, 3 and 4 splice variants of hBest3 mRNA (encoding protein isoforms 1, 3 and 4, respectively). Variant 1 represents the longest, full-length transcript for hBest3 gene (protein product 668aa), variant 3 lacks exons 2 and 3 (562aa) and variant 4 lacks a big part of exon 10 (398aa).

Variant 1 corresponds to the full-length protein of hBest3 with all predicted transmembrane domains present, and as the transmembrane area is highly conserved between all bestrophins and between the species, such a protein will most likely be able to function as an ion channel. The relevant model in rodents is mouse heart tissue, where mBest3 was shown to be expressed as full-length mRNA, and where Best3-related CAC current was observed in cardiac myocytes (62). Rat vascular smooth muscle is another tissue where mBest3 is responsible for a CAC channel *in vivo*, so we expect to see the full-length mRNA and protein expressed there, but the analysis of splicing in rat tissues, and in particular in rat vasculature, has not been done yet.

Variant 4 of hBest3 mRNA does not have analogs in mouse and encodes a protein that has an intact pore-forming region, but lacks most of the C-terminal part. Such a splice variant of hBest3 will keep the structural features of an ion channel. Some of the regulatory areas

of C-terminus, such as calcium-sensing domain and autoinhibitory regions, will be kept, but some will be missing, e.g. predicted PKG-phosphorylation sites mostly localized in the last two-thirds of C-terminus (Fig.7). *In-silico* analysis of the protein structure of the rat, mouse and human C-terminus predicted potential phosphorylation sites for PKG (see Paper I, Supplement and Fig.7 A), so phosphorylation of the C-terminal part of Best3 might be involved in regulation of Best3 protein function, probably due to the phosphorylation-induced conformational changes. On the other hand regulation of Best3 protein by cGMP might be indirect, but in rat tissue it is still due to PKG-dependent phosphorylation, as inactivation of PKG made regulation of the Best3-related current by cGMP impossible (Paper I). In mouse C-terminus 65% of protein is predicted by the Phyre2 algorithm to be disordered (42), which makes it difficult to model its 3D structure. Some other variants of regulation of Best3 can be suggested, including proteolytic cleavage of the C-terminus; if so one could speculate of an independent function of the cleaved fragment, as it happens for L-type calcium channels (34).

Variant 3 of hBest3 mRNA translates into a truncated protein lacking a part of the pore-forming transmembrane region of the channel, so it is unlikely that it is able to function as a channel. This variant of hBest3 is similar to mouse "-2-3+6" variant, which we found to be involved in cellular responses to injury and which might participate in a possible cell-protective action of Best3. At the same time the calcium-sensing area, the area responsible for an autoinhibitory action of the C-terminus and the predicted phosphorylation sites for PKG are intact in such proteins and might also participate in regulation of its function.

Different functional aspects have been studied in different species, and since it is not clear whether splicing varies between species it is difficult to draw conclusions from the data. In the rat cGMP-activated CAC current was also observed in renal proximal tubule cells (25), where later rBest3 was shown to participate in cell protection against ER stress (49). This might mean that in rat tissues anti-apoptotic functions of Best3 are related to its activity as a channel or to its sensitivity to cGMP. At the same time another CAC channel, anoctamin-1, is expressed in human and mouse proximal tubules (with

some expression observed also in podocytes) (31) and in mouse collecting duct (91), which might mean that anoctamin-1 and Best3 may collaborate in these tissues, if Best3 is a cGMP-sensitive regulator for anoctamin-1.

Expression of Best3 in human tissues

Best3 in human tissues is very little studied, and it is reported and characterized only on mRNA level in very few publications. The most detailed study of Best3 expression in humans is made by Stöhr and co-authors (86) where they detected hBest3 mRNA in skeletal muscle, brain, spinal cord, bone marrow and retina, thymus and testis and also described the presence of alternative splicing of hBest3 mRNA. Best3 mRNA was also detected in human heart (62). Our unpublished observations (see reference in Paper II) showed presence of Best3 mRNA in human kidney homogenate. No function for Best3 protein has been reported in humans *in vivo*. However, the well-proven involvement of Best3 in cGMP-regulated CAC current in rat vascular smooth muscle, and also increasing data on cell-protective and anti-apoptotic functions of Best3 in rat and mouse cells and tissues suggest that similar studies in human tissues are of great interest. Such studies may open for novel future applications to human diseases associated with ER stress and inflammation.

Our analysis of the literature shows that in humans Best3 protein might exist in variants with the transmembrane part intact and thus can be functioning as an ion channel. As the C-terminus in these proteins can be present or truncated, their regulation and channel properties can be different. Human Best3 mRNA can also be spliced with the loss of the exons corresponding to the transmembrane region of the protein, so proteins produced in this case will likely be lacking channel functions. We believe that in the studies of human Best3 function, the mouse would be a relevant model for studying functions of truncated splice variants of Best3, and the rat models might be used for studying cGMP-associated channel function of full-length Best3 protein.

6 CONCLUSIONS

Bestrophin-3 is a multifaceted protein. Like the other bestrophins it can constitute a chloride channel. In particular, as shown in Paper I, it participates in forming a cGMP-dependent, calcium-activated chloride channel in vascular smooth muscle in the rat. Bestrophin-3 is important for coupling changes in intracellular calcium to NO/cGMP pathway and for synchronizing the phasic activity of vascular smooth muscle cells. In other tissues in mouse (Paper II, III and IV), alternative splicing causes formation of truncated variants of the protein that do not form ion channels, but rather have an intracellular localization. These variants are expressed in mouse in podocytes in kidney glomeruli (Paper II), in astrocytes in neonatal brain after hypoxia-ischemia (Paper III), and in glia-like cells in the myenteric plexus of the intestine (Paper IV) — three cell types that may have common features. In particular, the distribution of bestrophin-3 here seems to follow that of the intermediate filament nestin. Bestorphin-3 also is expressed in ependymal cells of the brain ventricles (Paper III) and in goblet cells in the intestine (Paper IV). The expression of Best3 changes in response to LPS-induced inflammation and in response to endoplasmic reticulum stress (Paper II and III). Under these conditions, alternative splicing is altered, causing the expression of the individual splice variants to follow separate time courses. It is suggested that the changes in splicing and in the ratio between the splice variants, are important for the cellular response to stress. Alternative splicing may explain the variation in function of Best3. The physiological and pathophysiological roles of bestrophin-3 thus deserve further study.

ACKNOWLEDGEMENTS

I would like to express my sincere gratitude, love and appreciation to all the wonderful people I met at department of Physiology during my PhD studies, to those whom I worked with and laughed with. We shared happy moments, and you supported me during difficult times, and without you, my dearest colleagues and friends, there would have been no inspiration!

In particular, I would like to thank:

- My supervisor Helena Gustafsson - for your friendship and always positive attitude, for your help and trust and for our great evenings with you and your family!

- My co-supervisor Carina Mallard – for your warm support, for your great sense of humor, for always having time to listen and to talk and for being there for me when I felt lonely or panicked!

- Colleagues and friends from the group (family!) of Henrik Hagberg and Carina Mallard for helping me so much with my project, for teaching me many new tings and just for being such good friends: Anna-Lena Leverin (for your smile and saying "But it's easy!"), Pernilla Svedin (for your listening and understanding), Ana Baburamani (for being our Sunshine independently of weather or life storms), Pete Smith (for your great friendship, understanding, support and guitar lessons!), Anna-Maj Albertsson and Amin Mottahedin for our laughters in EBM during those strange working hours, Joakim Ek (you are just so nice, always!), Linnea Stridh for our fun conversaions, Xiaoyang Wang, Barbara DiAngelo, Gabriella Koning, Syam Nair, Nina Erkenstam, Kristina Sobotka.

- Collegues and friends from the groups of Jenny Nyström and Börje Haraldsson for helping me with my research in kidney, but also for accepting me in your nice family and for our great times together after work. Jenny, Börje, Johannes Elvin, Lisa Buvall, Hanna Wallentin, Heidi Hedman, and my dear friends Kerstin Ebefors (life is never boring when you are around!) and Peidi Liu (you are a great officemate and a genuinely kind person!).

- Collegues and friends from Maria Johansson's group (also a family!) for being so close, so nice, so helpful and so fun! Maria, you are such a great person, you are always ready to help, and your advices, as well as your funny comments, many times rescued my day. Marcus Ulleryd, Peter Micaleff, Sansan Hua, Li Jin Yang, Sara Svahn – we had so many good moments together, many cakes eaten, many events celebrated, but also some sad moments survived through together with you all!

- Collegues and friends from Holger Nilsson's group: Lisa Nguy (you are so fun, we all miss you, come back!), Emman Shubar (you are absolutely fantastic person!), our wonderful girls Marta Laskowski, Emilie Eliasson, Cathrin Andersson and Ida Carlsson – you bring to the lab so much joy, happiness, laughter, mess, action, life. Summer is the best time of the year also because then you all are in the lab together.

I would also give my special thanks to Kerstin Hörnberg – you helped me so many times with so many things, you gave me so much warmth and support when I needed it!

Many thanks to many great people from our institute, whom it was always nice to see –Eric Hanse, Ingela Hammar, Mats Sandberg, Rita Grandér, Lars Stage, Peter Thorén, Marja Bosaeus.

I would also like to thank colleagues from Astra-Zeneca - Ulla Brandt-Elliasson, Martin Kjerrulf, Ann-Cathrine Jonsson-Rylander and Julia Grönros, it was pleasure to work with you!

My very special thanks are also to Christian Aalkajer's group in Aarhus university in Denmark, where we spent unforgettable two and a half years, where the bestrophin-3 project started and developed. My dear Vladimir Matchkov and Elena Bouzinova, Christian Aalkajer, Jørgen Andresen and Susie Mogensen, I love you and miss you! Those years were special – difficult and happy at the same time, and thanks to you there always was hope and light.

Of course, I also want to thank my wonderful family – my mother, father, Sveta and Misha, and also my best friends – Nastya and Mila. Nothing is possible without your love, support, patience,

understanding, listening, forgiving… Thank you for being with me in good and bad moments and simply for being you.

And finally – Holger, my dearest husband, best friend and collaborator, thank you for helping me through this period of completing my thesis by being there, by being you – loving, patient, smart. Your sense of humor is always refreshing, and your ability to analyze things and to see the whole picture is great. Without you I would have been just another hopeless designer, but not a 2xPhD... ;)

REFERENCES

1. **Aalkjær C and Nilsson H**. Vasomotion: cellular background for the oscillator and for the synchronization of smooth muscle cells. *Br J Pharmacol* 144: 605-616, 2005.
2. **Abdallah Y, Kasseckert SA, Iraqi W, Said M, Shahzad T, Erdogan A, Neuhof C, Gunduz D, Schluter KD, Tillmanns H, Piper HM, Reusch HP and Ladilov Y**. Interplay between Ca^{2+} cycling and mitochondrial permeability transition pores promotes reperfusion-induced injury of cardiac myocytes. *J Cell Mol Med* 15: 2478-2485, 2011.
3. **Akgul C, Moulding DA and Edwards SW**. Alternative splicing of Bcl-2-related genes: functional consequences and potential therapeutic applications. *Cell Mol Life Sci* 61: 2189-2199, 2004.
4. **Aldehni F, Spitzner M, Martins JR, Barro-Soria R, Schreiber R and Kunzelmann K**. Bestrophin 1 promotes epithelial-to-mesenchymal transition of renal collecting duct cells. *J Am Soc Nephrol* 20: 1556-1564, 2009.
5. **Bader CR, Bertrand D and Schwartz EA**. Voltage-activated and calcium-activated currents studied in solitary rod inner segments from the salamander retina. *J Physiol* 331: 253-284, 1982.
6. **Bakall B, McLaughlin P, Stanton JB, Zhang Y, Hartzell HC, Marmorstein LY and Marmorstein AD**. Bestrophin-2 is involved in the generation of intraocular pressure. *Invest Ophthalmol Vis Sci* 49: 1563-1570, 2008.
7. **Banas MC, Banas B, Hudkins KL, Wietecha TA, Iyoda M, Bock E, Hauser P, Pippin JW, Shankland SJ, Smith KD, Stoelcker B, Liu G, Grone HJ, Krämer F and Alpers CE**. TLR4 links podocytes with the innate immune system to mediate glomerular injury. *J Am Soc Nephrol* 19: 704-713, 2008.
8. **Barro-Soria R, Aldehni F, Almaca J, Witzgall R, Schreiber R and Kunzelmann K**. ER-localized bestrophin 1 activates Ca^{2+}-

dependent ion channels TMEM16A and SK4 possibly by acting as a counterion channel. *Pflügers Arch* 459: 485-497, 2010.

9. **Benavides A, Pastor D, Santos P, Tranque P and Calvo S**. CHOP plays a pivotal role in the astrocyte death induced by oxygen and glucose deprivation. *Glia* 52: 261-275, 2005.
10. **Bertelli E, Regoli M, Fonzi L, Occhini R, Mannucci S, Ermini L and Toti P**. Nestin expression in adult and developing human kidney. *J Histochem Cytochem* 55: 411-421, 2007.
11. **Bharill S, Fu Z, Palty R and Isacoff EY**. Stoichiometry and specific assembly of Best ion channels. *Proc Natl Acad Sci U S A* 111: 6491-6496, 2014.
12. **Boudes M, Sar C, Menigoz A, Hilaire C, Pequignot MO, Kozlenkov A, Marmorstein A, Carroll P, Valmier J and Scamps F**. Best1 is a gene regulated by nerve injury and required for Ca^{2+}-activated Cl^- current expression in axotomized sensory neurons. *J Neurosci* 29: 10063-10071, 2009.
13. **Brinkkoetter PT, Olivier P, Wu JS, Henderson S, Krofft RD, Pippin JW, Hockenbery D, Roberts JM and Shankland SJ**. Cyclin I activates Cdk5 and regulates expression of Bcl-2 and Bcl-XL in postmitotic mouse cells. *J Clin Invest* 119: 3089-3101, 2009.
14. **Broegger T, Jacobsen JC, Secher D, V, Boedtkjer DM, Kold-Petersen H, Pedersen FS, Aalkjaer C and Matchkov VV**. Bestrophin is important for the rhythmic but not the tonic contraction in rat mesenteric small arteries. *Cardiovasc Res* 91: 685-693, 2011.
15. **Buniatian G, Traub P, Albinus M, Beckers G, Buchmann A, Gebhardt R and Osswald H**. The immunoreactivity of glial fibrillary acidic protein in mesangial cells and podocytes of the glomeruli of rat kidney in vivo and in culture. *Biol Cell* 90: 53-61, 1998.
16. **Buniatian GH, Hartmann HJ, Traub P, Wiesinger H, Albinus M, Nagel W, Shoeman R, Mecke D and Weser U**. Glial fibrillary

acidic protein-positive cells of the kidney are capable of raising a protective biochemical barrier similar to astrocytes: expression of metallothionein in podocytes. *Anat Rec* 267: 296-306, 2002.

17. **Byrne NG and Large WA**. Membrane ionic mechanisms activated by noradrenaline in cells isolated from the rabbit portal vein. *J Physiol* 404: 557-573, 1988.
18. **Cantarero Carmona I, Luesma Bartolomé MJ, Lavoie-Gagnon C and Junquera Escribano C.** Distribution of nestin protein: immunohistochemical study in enteric plexus of rat duodenum. *Microsc Res Tech* 74: 148-152, 2011.
19. **Caputo A, Caci E, Ferrera L, Pedemonte N, Barsanti C, Sondo E, Pfeffer U, Ravazzolo R, Zegarra-Moran O and Galietta LJ**. TMEM16A, a membrane protein associated with calcium-dependent chloride channel activity. *Science* 322: 590-594, 2008.
20. **Carloni S, Albertini MC, Galluzzi L, Buonocore G, Proietti F and Balduini W**. Increased autophagy reduces endoplasmic reticulum stress after neonatal hypoxia-ischemia: role of protein synthesis and autophagic pathways. *Exp Neurol* 255: 103-112, 2014.
21. **Chien LT, Zhang ZR and Hartzell HC**. Single Cl^- channels activated by Ca^{2+} in Drosophila S2 cells are mediated by bestrophins. *J Gen Physiol* 128: 247-259, 2006.
22. **Cho JM, Shin YJ, Park JM, Kim J and Lee MY**. Characterization of nestin expression in astrocytes in the rat hippocampal CA1 region following transient forebrain ischemia. *Anat Cell Biol* 46: 131-140, 2013.
23. **Comper WD**. Is the LPS-mediated proteinuria mouse model relevant to human kidney disease? *Nat Med* 15: 133-134, 2009.
24. **Dam VS, Boedtkjer DM, Nyvad J, Aalkjaer C and Matchkov V**. TMEM16A knockdown abrogates two different Ca^{2+}-activated Cl^- currents and contractility of smooth muscle in rat mesenteric small arteries. *Pflugers Arch* 466: 1391-1409, 2014.

25. **Darvish N, Winaver J and Dagan D**. A novel cGMP-activated Cl^- channel in renal proximal tubules. *Am J Physiol* 268: F323-F329, 1995.

26. **de Vellis J, Ghiani CA, Wanner IB and Cole R**. Preparation of Normal and Reactive Astrocyte Cultures. In: Protocols for Neural Cell Culture, edited by Doering LC. Humana Press, 2010, p. 193-215.

27. **Duran C, Thompson CH, Xiao Q and Hartzell HC**. Chloride channels: often enigmatic, rarely predictable. *Annu Rev Physiol* 72: 95-121, 2010.

28. **Duta V, Duta F, Puttagunta L, Befus AD and Duszyk M**. Regulation of basolateral Cl^- channels in airway epithelial cells: the role of nitric oxide. *J Membr Biol* 213: 165-174, 2006.

29. Ek, C. J., D'Angelo, B., Baburamani, A., Lehner, C., Leverin, A.-L., Smith, P., Nilsson, H., Svedin, P., Hagberg, H., and Mallard, C. Brain barrier properties and cerebral blood flow in neonatal mice exposed to cerebral hypoxia-ischemia. J.Cereb.Blood Flow Metab . 2015. Ref Type: In Press

30. **Esposito V, Grosjean F, Tan J, Huang L, Zhu L, Chen J, Xiong H, Striker GE and Zheng F**. CHOP deficiency results in elevated lipopolysaccharide-induced inflammation and kidney injury. *Am J Physiol Renal Physiol* 304: F440-F450, 2013.

31. **Faria D, Rock JR, Romao AM, Schweda F, Bandulik S, Witzgall R, Schlatter E, Heitzmann D, Pavenstädt H, Herrmann E, Kunzelmann K and Schreiber R**. The calcium-activated chloride channel Anoctamin 1 contributes to the regulation of renal function. *Kidney Int* 85: 1369-1381, 2014.

32. **Fischmeister R and Hartzell HC**. Volume sensitivity of the bestrophin family of chloride channels. *J Physiol* 562: 477-491, 2005.

33. **Gilyarov AV**. Nestin in central nervous system cells. *Neurosci Behav Physiol* 38: 165-169, 2008.

34. **Gomez-Ospina N, Tsuruta F, Barreto-Chang O, Hu L and Dolmetsch R**. The C terminus of the L-type voltage-gated calcium channel $Ca_V1.2$ encodes a transcription factor. *Cell* 127: 591-606, 2006.

35. **Gustafsson H**. Vasomotion and underlying mechanisms in small arteries. *Acta Physiol Scand* 149 (Suppl. 614): 1-44, 1993.

36. **Gustafsson H, Mulvany MJ and Nilsson H**. Rhythmic contractions of isolated small arteries from rat: influence of the endothelium. *Acta Physiol Scand* 148: 153-163, 1993.

37. **Hartzell HC, Qu Z, Yu K, Xiao Q and Chien LT**. Molecular physiology of bestrophins: multifunctional membrane proteins linked to best disease and other retinopathies. *Physiol Rev* 88: 639-672, 2008.

38. **Jentsch TJ, Stein V, Weinreich F and Zdebik AA**. Molecular structure and physiological function of chloride channels. *Physiol Rev* 82: 503-568, 2002.

39. **Jiang L, Liu Y, Ma MM, Tang YB, Zhou JG and Guan YY**. Mitochondria dependent pathway is involved in the protective effect of bestrophin-3 on hydrogen peroxide-induced apoptosis in basilar artery smooth muscle cells. *Apoptosis* 18: 556-565, 2013.

40. **Kane Dickson V, Pedi L and Long SB**. Structure and insights into the function of a Ca^{2+}-activated Cl^- channel. *Nature* 516: 213-218, 2014.

41. **Kaneko Y, Tajiri N, Yu S, Hayashi T, Stahl CE, Bae E, Mestre H, Franzese N, Rodrigues A, Jr., Rodrigues MC, Ishikawa H, Shinozuka K, Hethorn W, Weinbren N, Glover LE, Tan J, Achyuta AH, van LH, Sanberg PR, Shivsankar S and Borlongan CV**. Nestin overexpression precedes caspase-3 upregulation in rats exposed to controlled cortical impact traumatic brain injury. *Cell Med* 4: 55-63, 2012.

42. **Kelley LA and Sternberg MJ**. Protein structure prediction on the Web: a case study using the Phyre server. *Nat Protoc* 4: 363-371, 2009.

43. **Kimes BW and Brandt BL**. Characterization of two putative smooth muscle cell lines from rat thoracic aorta. *Exp Cell Res* 98: 349-366, 1976.

44. **Klimmeck D, Daiber PC, Bruhl A, Baumann A, Frings S and Mohrlen F**. Bestrophin 2: an anion channel associated with neurogenesis in chemosensory systems. *J Comp Neurol* 515: 585-599, 2009.

45. **Krämer F, Stöhr H and Weber BH**. Cloning and characterization of the murine Vmd2 RFP-TM gene family. *Cytogenet Genome Res* 105: 107-114, 2004.

46. **Krogh A, Larsson B, von Heijne G. and Sonnhammer EL**. Predicting transmembrane protein topology with a hidden Markov model: application to complete genomes. *J Mol Biol* 305: 567-580, 2001.

47. **Kuo YH, Abdullaev IF, Hyzinski-Garcia MC and Mongin AA**. Effects of alternative splicing on the function of bestrophin-1 calcium-activated chloride channels. *Biochem J* 458: 575-583, 2014.

48. **Lee S, Yoon BE, Berglund K, Oh SJ, Park H, Shin HS, Augustine GJ and Lee CJ**. Channel-mediated tonic GABA release from glia. *Science* 330: 790-796, 2010.

49. **Lee WK, Chakraborty PK, Roussa E, Wolff NA and Thevenod F**. ERK1/2-dependent bestrophin-3 expression prevents ER-stress-induced cell death in renal epithelial cells by reducing CHOP. *Biochim Biophys Acta* 1823: 1864-1876, 2012.

50. **Liu W, Zhang Y, Hao J, Liu S, Liu Q, Zhao S, Shi Y and Duan H**. Nestin protects mouse podocytes against high glucose-induced apoptosis by a Cdk5-dependent mechanism. *J Cell Biochem* 113: 3186-3196, 2012.

51. **Liu W, Zhang Y, Liu S, Liu Q, Hao J, Shi Y, Zhao S and Duan H**. The expression of intermediate filament protein nestin and its association with cyclin-dependent kinase 5 in the glomeruli of rats with diabetic nephropathy. *Am J Med Sci* 345: 470-477, 2013.

52. **Marmorstein AD and Marmorstein LY**. The challenge of modeling macular degeneration in mice. *Trends Genet* 23: 225-231, 2007.

53. **Marmorstein LY, McLaughlin PJ, Stanton JB, Yan L, Crabb JW and Marmorstein AD**. Bestrophin interacts physically and functionally with protein phosphatase 2A. *J Biol Chem* 277: 30591-30597, 2002.

54. **Marmorstein LY, Wu J, McLaughlin P, Yocom J, Karl MO, Neussert R, Wimmers S, Stanton JB, Gregg RG, Strauss O, Peachey NS and Marmorstein AD**. The light peak of the electroretinogram is dependent on voltage-gated calcium channels and antagonized by bestrophin (best-1). *J Gen Physiol* 127: 577-589, 2006.

55. **Matchkov V, Aalkjær C and Nilsson H**. A cyclic-GMP-dependent calcium-activated chloride current in smooth muscle cells from rat mesenteric resistance arteries. *J Gen Physiol* 123: 121-134, 2004.

56. **Matchkov VV, Aalkjaer C and Nilsson H**. Distribution of cGMP-dependent and cGMP-independent Ca^{2+}-activated Cl^- conductances in smooth muscle cells from different vascular beds and colon. *Pflügers Arch* 451: 371-379, 2005.

57. **Milenkovic VM, Krejcova S, Reichhart N, Wagner A and Strauss O**. Interaction of bestrophin-1 and Ca^{2+} channel b-subunits: identification of new binding domains on the bestrophin-1 C-terminus. *PLoS One* 6: e19364, 2011.

58. **Mundel P, Reiser J and Kriz W**. Induction of differentiation in cultured rat and human podocytes. *J Am Soc Nephrol* 8: 697-705, 1997.

59. **Mundel P, Reiser J, Zuniga Mejia BA, Pavenstädt H, Davidson GR, Kriz W and Zeller R**. Rearrangements of the cytoskeleton and cell contacts induce process formation during differentiation of conditionally immortalized mouse podocyte cell lines. *Exp Cell Res* 236: 248-258, 1997.

60. **Neussert R, Muller C, Milenkovic VM and Strauss O**. The presence of bestrophin-1 modulates the Ca^{2+} recruitment from Ca^{2+} stores in the ER. *Pflügers Arch* 460: 163-175, 2010.

61. **Nilsson H and Aalkjaer C**. Vasomotion: mechanisms and physiological importance. *Mol Interventions* 3: 79-89, 2003.

62. **O'Driscoll KE, Hatton WJ, Burkin HR, Leblanc N and Britton FC**. Expression, localization, and functional properties of Bestrophin 3 channel isolated from mouse heart. *Am J Physiol Cell Physiol* 295: C1610-C1624, 2008.

63. **Oh SJ, Han KS, Park H, Woo DH, Kim HY, Traynelis SF and Lee CJ**. Protease activated receptor 1-induced glutamate release in cultured astrocytes is mediated by Bestrophin-1 channel but not by vesicular exocytosis. *Mol Brain* 5: 38, 2012.

64. **Oikawa H, Hayashi K, Maesawa C, Masuda T and Sobue K**. Expression profiles of nestin in vascular smooth muscle cells in vivo and in vitro. *Exp Cell Res* 316: 940-950, 2010.

65. **Oyadomari S and Mori M**. Roles of CHOP/GADD153 in endoplasmic reticulum stress. *Cell Death Differ* 11: 381-389, 2004.

66. **Peng HL, Matchkov V, Ivarsen A, Aalkjær C and Nilsson H**. Hypothesis for the initiation of vasomotion. *Circ Res* 88: 810-815, 2001.

67. **Petrukhin K, Koisti MJ, Bakall B, Li W, Xie G, Marknell T, Sandgren O, Forsman K, Holmgren G, Andreasson S, Vujic M, Bergen AA, McGarty-Dugan V, Figueroa D, Austin CP, Metzker ML, Caskey CT and Wadelius C**. Identification of the gene responsible for Best macular dystrophy. *Nat Genet* 19: 241-247, 1998.

68. **Piper AS and Large WA**. Single cGMP-activated Ca^{2+}-dependent Cl^- channels in rat mesenteric artery smooth muscle cells. *J Physiol* 555: 397-408, 2004.

69. **Poltorak A, He X, Smirnova I, Liu MY, Van HC, Du X, Birdwell D, Alejos E, Silva M, Galanos C, Freudenberg M, Ricciardi-Castagnoli P, Layton B and Beutler B**. Defective LPS signaling in C3H/HeJ and C57BL/10ScCr mice: mutations in Tlr4 gene. *Science* 282: 2085-2088, 1998.

70. **Prell T, Lautenschläger J, Weidemann L, Ruhmer J, Witte OW and Grosskreutz J**. Endoplasmic reticulum stress is accompanied by activation of NF-kB in amyotrophic lateral sclerosis. *J Neuroimmunol* 270: 29-36, 2014.

71. **Qu Z, Han X, Cui Y and Li C**. A PI3 kinase inhibitor found to activate bestrophin 3. *J Cardiovasc Pharmacol* 55: 110-115, 2010.

72. **Qu Z and Hartzell HC**. Bestrophin Cl^- channels are highly permeable to $HCO3^-$. *Am J Physiol Cell Physiol* 294: C1371-C1377, 2008.

73. **Qu ZQ, Yu K, Cui YY, Ying C and Hartzell C**. Activation of bestrophin Cl- channels is regulated by C-terminal domains. *J Biol Chem* 282: 17460-17467, 2007.

74. **Reiser J, von GG, Loos M, Oh J, Asanuma K, Giardino L, Rastaldi MP, Calvaresi N, Watanabe H, Schwarz K, Faul C, Kretzler M, Davidson A, Sugimoto H, Kalluri R, Sharpe AH, Kreidberg JA and Mundel P**. Induction of B7-1 in podocytes is associated with nephrotic syndrome. *J Clin Invest* 113: 1390-1397, 2004.

75. **Rice JE, III, Vannucci RC and Brierley JB**. The influence of immaturity on hypoxic-ischemic brain damage in the rat. *Ann Neurol* 9: 131-141, 1981.

76. **Rosenthal R, Bakall B, Kinnick T, Peachey N, Wimmers S, Wadelius C, Marmorstein A and Strauss O**. Expression of bestrophin-1, the product of the VMD2 gene, modulates voltage-

dependent Ca2+ channels in retinal pigment epithelial cells. *FASEB J* 20: 178-180, 2006.

77. **Schroeder BC, Cheng T, Jan YN and Jan LY**. Expression cloning of TMEM16A as a calcium-activated chloride channel subunit. *Cell* 134: 1019-1029, 2008.
78. **Shankland SJ, Pippin JW, Reiser J and Mundel P**. Podocytes in culture: past, present, and future. *Kidney Int* 72: 26-36, 2007.
79. **Sheldon RA, Sedik C and Ferriero DM**. Strain-related brain injury in neonatal mice subjected to hypoxia-ischemia. *Brain Res* 810: 114-122, 1998.
80. **Shi SR, Chaiwun B, Young L, Cote RJ and Taylor CR**. Antigen retrieval technique utilizing citrate buffer or urea solution for immunohistochemical demonstration of androgen receptor in formalin-fixed paraffin sections. *J Histochem Cytochem* 41: 1599-1604, 1993.
81. **Shi SR, Imam SA, Young L, Cote RJ and Taylor CR**. Antigen retrieval immunohistochemistry under the influence of pH using monoclonal antibodies. *J Histochem Cytochem* 43: 193-201, 1995.
82. **Sizonenko SV, Camm EJ, Dayer A and Kiss JZ**. Glial responses to neonatal hypoxic-ischemic injury in the rat cerebral cortex. *Int J Dev Neurosci* 26: 37-45, 2008.
83. **Song W, Yang Z and He B**. Bestrophin 3 ameliorates TNFa-induced inflammation by inhibiting NF-kB activation in endothelial cells. *PLoS One* 9: e111093, 2014.
84. **Spitzner M, Martins JR, Soria RB, Ousingsawat J, Scheidt K, Schreiber R and Kunzelmann K**. Eag1 and Bestrophin 1 are up-regulated in fast-growing colonic cancer cells. *J Biol Chem* 283: 7421-7428, 2008.
85. **Srivastava A, Romanenko VG, Gonzalez-Begne M, Catalan MA and Melvin JE**. A variant of the Ca^{2+}-activated Cl channel Best3 is expressed in mouse exocrine glands. *J Membr Biol* 222: 43-54, 2008.

86. **Stöhr H, Marquardt A, Nanda I, Schmid M and Weber BH**. Three novel human VMD2-like genes are members of the evolutionary highly conserved RFP-TM family. *Eur J Hum Genet* 10: 281-284, 2002.

87. **Strauss O, Müller C, Reichhart N, Tamm ER and Gomez NM**. The role of bestrophin-1 in intracellular Ca^{2+} signaling. *Adv Exp Med Biol* 801: 113-119, 2014.

88. **Su W, Chen J, Yang H, You L, Xu L, Wang X, Li R, Gao L, Gu Y, Lin S, Xu H, Breyer MD and Hao CM**. Expression of nestin in the podocytes of normal and diseased human kidneys. *Am J Physiol Regul Integr Comp Physiol* 292: R1761-R1767, 2007.

89. **Sun H, Tsunenari T, Yau KW and Nathans J**. The vitelliform macular dystrophy protein defines a new family of chloride channels. *Proc Natl Acad Sci U S A* 99: 4008-4013, 2002.

90. **Suzuki T, Sakata H, Kato C, Connor JA and Morita M**. Astrocyte activation and wound healing in intact-skull mouse after focal brain injury. *Eur J Neurosci* 36: 3653-3664, 2012.

91. **Svenningsen P, Nielsen MR, Marcussen N, Walter S and Jensen BL**. TMEM16A is a Ca^{2+} -activated Cl^- channel expressed in the renal collecting duct. *Acta Physiol (Oxf)* 212: 166-174, 2014.

92. **Tan Y and Kagan JC**. A cross-disciplinary perspective on the innate immune responses to bacterial lipopolysaccharide. *Mol Cell* 54: 212-223, 2014.

93. **Tochitani S and Kondo S**. Immunoreactivity for GABA, GAD65, GAD67 and Bestrophin-1 in the meninges and the choroid plexus: implications for non-neuronal sources for GABA in the developing mouse brain. *PLoS One* 8: e56901, 2013.

94. **Tsunenari T, Nathans J and Yau KW**. Ca^{2+}-activated Cl^- current from human bestrophin-4 in excised membrane patches. *J Gen Physiol* 127: 749-754, 2006.

95. **Tsunenari T, Sun H, Williams J, Cahill H, Smallwood P, Yau KW and Nathans J**. Structure-function analysis of the bestrophin family of anion channels. *J Biol Chem* 2003.

96. **Urban P, Pavlikova M, Sivonova M, Kaplan P, Tatarkova Z, Kaminska B and Lehotsky J**. Molecular analysis of endoplasmic reticulum stress response after global forebrain ischemia/reperfusion in rats: effect of neuroprotectant simvastatin. *Cell Mol Neurobiol* 29: 181-192, 2009.

97. **Vannucci SJ and Hagberg H**. Hypoxia-ischemia in the immature brain. *J Exp Biol* 207: 3149-3154, 2004.

98. **Wagner N, Wagner KD, Scholz H, Kirschner KM and Schedl A**. Intermediate filament protein nestin is expressed in developing kidney and heart and might be regulated by the Wilms' tumor suppressor Wt1. *Am J Physiol Regul Integr Comp Physiol* 291: R779-R787, 2006.

99. **Wen D, You L, Zhang Q, Zhang L, Gu Y, Hao CM and Chen J**. Upregulation of nestin protects podocytes from apoptosis induced by puromycin aminonucleoside. *Am J Nephrol* 34: 423-434, 2011.

100. **Xiao Q, Ford AL, Xu J, Yan P, Lee KY, Gonzales E, West T, Holtzman DM and Lee JM**. Bcl-x pre-mRNA splicing regulates brain injury after neonatal hypoxia-ischemia. *J Neurosci* 32: 13587-13596, 2012.

101. **Xiao Q, Prussia A, Yu K, Cui YY and Hartzell HC**. Regulation of bestrophin Cl channels by calcium: role of the C terminus. *J Gen Physiol* 132: 681-692, 2008.

102. **Xu C, Bailly-Maitre B and Reed JC**. Endoplasmic reticulum stress: cell life and death decisions. *J Clin Invest* 115: 2656-2664, 2005.

103. **Xue Y, Zhou F, Zhu M, Ahmed K, Chen G and Yao X**. GPS: a comprehensive www server for phosphorylation sites prediction. *Nucleic Acids Res* 33: W184-W187, 2005.

104. **Yang T, Liu Q, Kloss B, Bruni R, Kalathur RC, Guo Y, Kloppmann E, Rost B, Colecraft HM and Hendrickson WA**. Structure and selectivity in bestrophin ion channels. *Science* 346: 355-359, 2014.

105. **Yang YD, Cho H, Koo JY, Tak MH, Cho Y, Shim WS, Park SP, Lee J, Lee B, Kim BM, Raouf R, Shin YK and Oh U**. TMEM16A confers receptor-activated calcium-dependent chloride conductance. *Nature* 455: 1210-1215, 2008.

106. **Yu K, Lujan R, Marmorstein A, Gabriel S and Hartzell HC**. Bestrophin-2 mediates bicarbonate transport by goblet cells in mouse colon. *J Clin Invest* 120: 1722-1735, 2010.

107. **Yu K, Xiao Q, Cui G, Lee A and Hartzell HC**. The best disease-linked Cl^- channel hBest1 regulates Ca_V1 (L-type) Ca^{2+} channels via src-homology-binding domains. *J Neurosci* 28: 5660-5670, 2008.